

See discussions, stats, and author profiles for this publication at: <https://www.researchgate.net/publication/259621002>

# The Post-glacial Evolution of Chignecto Bay, Bay of Fundy, and its Modern Environment of Deposition

Chapter · March 1991

---

CITATIONS

32

READS

111

3 authors, including:



Carl L. Amos

University of Southampton

251 PUBLICATIONS 5,173 CITATIONS

SEE PROFILE

Some of the authors of this publication are also working on these related projects:

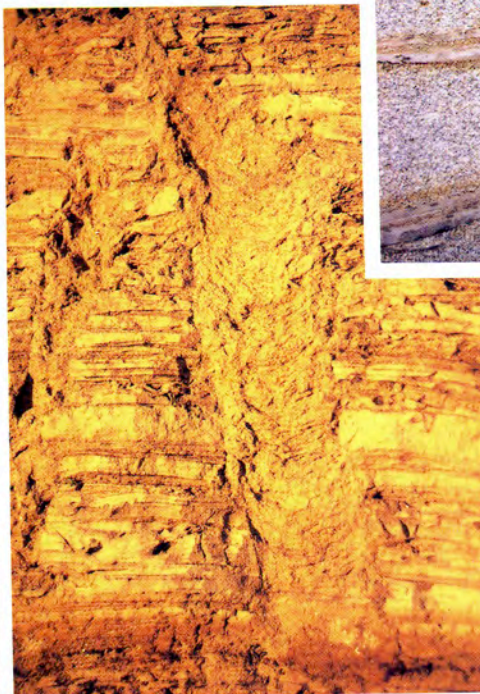
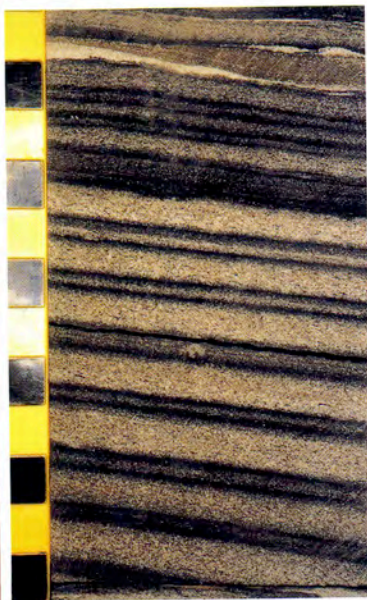
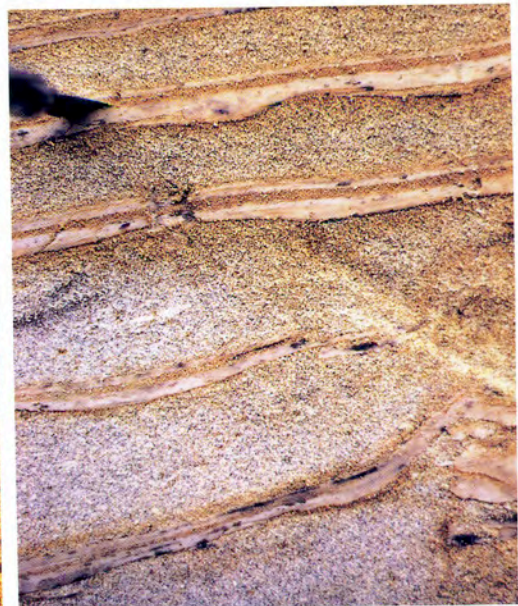
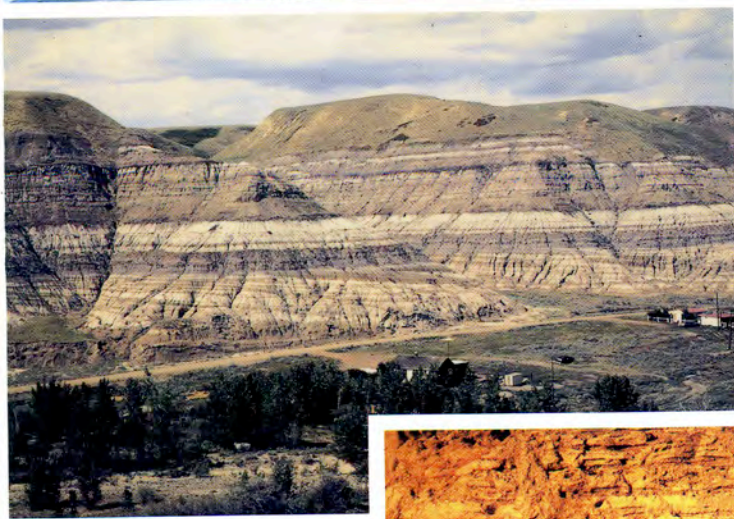


WAPOC - HYDRALAB III: Wave Propagation over Posidonia Oceanica [View project](#)



Bay of Fundy [View project](#)

# CLASTIC TIDAL SEDIMENTOLOGY



Edited by  
DERALD G. SMITH  
GERRY E. REINSON  
BRIAN A. ZAITLIN  
RAY A. RAHMANI

## The post-glacial evolution of Chignecto Bay, Bay of Fundy, and its modern environment of deposition

CARL L. AMOS

*Geological Survey of Canada  
Department of Energy, Mines and  
Resources  
Bedford Institute of Oceanography  
P.O. Box 1006, Dartmouth  
Nova Scotia, Canada  
B2Y 4A2*

KIM T. TEE

*Physical and Chemical Sciences  
Department of Fisheries and Oceans  
Bedford Institute of Oceanography  
P.O. Box 1006, Dartmouth  
Nova Scotia, Canada  
B2Y 4A2*

BRIAN A. ZAITLIN

*Esso Resources Canada Ltd.  
237, 4th Avenue S.W.  
Calgary, Alberta, Canada  
T2P 0H6*

### ABSTRACT

Chignecto Bay is a macrotidal estuary situated in the upper part of the upper Bay of Fundy. Its physiography is bedrock controlled though it is blanketed in the upper reaches by transgressive, silty, glacial and postglacial unconsolidated sediments. This sequence is largely preserved in the sublittoral portion of the bay. It is complicated by rapid changes in sea level (55 m above present sea level at 15,000 BP, 25 m below present sea level circa 7,000 BP) and large changes in tidal range (varying from less than 2 m to more than 12 m over the last 13,300 years). The fining-upward macrosequence and expansive sand flats, which typify wide, shallow, mesotidal and macrotidal estuaries such as Minas Basin, are largely absent due to the major changes in sea level and tidal range. The depositional character and trapping efficiency of the estuary has also changed dramatically. From 13,300 to 10,000 BP, the estuary was characterized by seabed erosion, by the dominance of macrotidal sand and gravel facies throughout the estuary, by a low trapping efficiency of fine grained sediment and by a net export of this material. Between 9,000 and 6,000 BP, the estuary was characterized by the rapid accumulation of sand/mud laminae in its central, eastern side, possibly within a mesotidal lagoon, and by a high trapping efficiency and a probable import of material suspended in the Bay of Fundy. Wave activity during this time was suppressed, possibly as a result of a barrier island across the mouth of the paleoestuary. The estuarine depocentre moved to the western side of the central and inner estuary between 6,000 and 3,000 BP. The dominant facies also changed to macrotidal lenticular and flaser bedding. From 3,000 BP to the present, the estuary returned to conditions interpreted as having prevailed during late Pleistocene. The depocentre for these Holocene sediments is along the eastern part of the central sublittoral estuary. Recent sublittoral sediments are dominated by sand and gravel facies. Recent littoral sediments form fringing mud flats and salt marshes in the inner estuary. The modern estuary is subject to a mean spring semidiurnal tidal range of 11.3 m and associated tidal currents in excess 1.5 m/s. These currents are eroding the previously-deposited muddy sediments and creating a transgressive sand unit dominated by large-scale bedforms (sand waves, 2-D and 3-D megaripples) and sand ribbons. The bay is presently exposed to a peak significant wave height of 2 m. Waves thus play a major role in reworking and resuspending seabed sediments and in releasing fine sand and silt ( $1.03 \times 10^6 \text{ m}^3/\text{a}$ ) through cliffline erosion (up to 1.0 m/a). A total of  $7.3 \times 10^6 \text{ m}^3$  of sediment is mobilized each year; 99 per cent of this volume is in the silt-clay size range and is transported in suspension. Residual circulation near the estuary mouth is headward along the eastern margins (0.1 m/s) and seaward along the western margin. Suspended sediment is transported out of the system as a result of this residual circulation ( $6.3 \times 10^6 \text{ m}^3/\text{a}$ ) and is subsequently deposited in the outer Bay of Fundy.

### RÉSUMÉ

La baie de Chignecto, située dans la partie supérieure de la baie de Fundy, est un estuaire macrotidal dont la physiographie est contrôlée par le substratum malgré le revêtement aux points culminants d'une séquence transgressive. Celle-ci, composée de sédiments glaciaires et post-glaciaires, silteux et non consolidés, est principalement préservée dans la zone sublittorale de la baie. Des changements rapides du niveau de la mer (55 m au-dessus du niveau actuel, il y a 15,000 av. P., et 25 m au-dessous du niveau actuel, il y a 7,000 av. P.) et des changements importants des écarts de marée (variation de moins de 2 m à plus de 12 m durant les derniers 13,300 ans) compliquent la séquence transgressive. La macroséquence virtuelle (i.e. granulométrie décroissante de la base au sommet) et les vastes estrans sableux («sand flats»), caractéristiques des estuaires, mesotidal et macrotidal, larges et peu profonds, comme par exemple le bassin Minas, sont absents principalement à cause des changements majeurs du niveau marin et des écarts de la marée. L'aspect sédimentaire et l'efficacité de piégeage des sédiments dans l'estuaire ont également changé drastiquement. Par exemple, de 13,300 à 10,000 ans av. P., l'estuaire se caractérisait par une érosion des couches marines, une prédominance des faciès macrotidaux sableux et graveleux, une faible efficacité du piégeage du sédiment fin et un transport net de ce sédiment fin vers l'extérieur du système. Par contre entre 9,000 et 6,000 ans av. P., la partie centrale-est de l'estuaire se caractérisait par une accumulation

Water samples were collected every two days for a period of approximately 9 months and analyzed by filtration for suspended sediment concentration and percentage of organic detritus. Coastal erosion was determined by comparison of orthophoto maps created from aerial photographs collected in 1947 and 1975, respectively. Volume input of sediment from this source was determined from cliff recession rates between the successive surveys and by scaling cliff height from large-format (105 mm), horizontal photographs of the cliffs. A review of the methods used, computational procedures, data collection and results is given in Hildebrand *et al.* (1980) and Amos and Asprey (1981).

#### REGIONAL SETTING AND GEOLOGICAL EVOLUTION

The Chignecto Bay system is subdivided into three physiographic provinces (Fig. 1): 1) Chignecto Bay, *sensu stricto*; 2) Shepody Bay; and 3) Cumberland Basin. A general summary of the dimensions of the Chignecto Bay system is given in Table 1. Chignecto Bay is a high-energy environment. It is dominated by semidiurnal tides that have a spring tidal range of 11.3 m and a neap tidal range of 7.2 m. The associated spring tidal prism is 5.56 km<sup>3</sup> causing peak currents between 1.0 and 2 m/s (Tee and Amos, *in press*). The bay is oriented parallel to the dominant northeast-southwest winds and is, therefore, subject to storm wave influences. This is apparent in its two coastal types: 1) a cliffed, high tide shoreline with a narrow intertidal zone in the central and outer parts of the estuary; and 2) a cliffed, salt marsh shoreline with an extensive intertidal zone in the inner parts of the estuary.

The gross morphology of Chignecto Bay is controlled by the Appalachian Orogenic Physiographic Province (Williams *et al.*, 1972), within which the bay is located. The system is largely controlled by development of the Chignecto-Chedabucto-Cobequid Fault Zone (C<sup>3</sup>FZ; Poole *et al.*, 1976). Post-Adian and Appalachian tectonic events (Carboniferous - Permian) along the C<sup>3</sup>FZ resulted in the formation of a series of semi-connected depositional basins infilled with terrestrial, shallow marine and volcanic material (Klein, 1970). The bedrock geology of the region exhibits Triassic half-graben basinal development, which began 430 million years ago (Swift and Lyall, 1968; Stephens, 1977). The half-graben was formed in Precambrian volcanics and Paleozoic fluvial and deltaic sediments and volcanics and was subsequently filled with Triassic sandstones and volcanics (King and MacLean, 1976). Bedrock flexuring during

earth movements upthrust and folded much of the material that presently forms the eroded cliffs at Chignecto Bay and underlies the bay. This material was further dissected by Cretaceous and Tertiary fluvial development (Grant, 1970).

The bedrock is composed of friable siltstone and shale that disintegrates to provide large quantities of silt-sized sediment to the bay. The character of the unconsolidated surficial sediments of Chignecto Bay thus reflects the lithology of the local bedrock, although it is modified in part by glacial erosion and postglacial tidal deposition. Fine grained (clay-rich) glacial and postglacial sediments or muddy gravel constitute much of the seabed of the outer Bay of Fundy and Chignecto Bay (Pelletier and McMullen, 1972; Swift *et al.*, 1973; Fader *et al.*, 1977). These sediments are presently in a state of erosion and are a source of the fine grained suspended sediments in the bay (Amos and Topliss, 1985; Tee and Amos, *in press*).

Shepody Bay and Cumberland Basin are separated from Chignecto Bay by constricted mouths at Cape Maringouin. These estuaries are characterized by highly turbid waters (Gordon and Dadswell, 1984; Amos and Asprey, 1981) and differ from Chignecto Bay by possessing extensive fringing salt marshes and mud flats (coastal type 2). These inner estuaries have been extensively modified during the last 13,300 years as a result of a period of regression and subsequent transgression and by large changes in tidal range. Much of the record of these events is preserved in the sublittoral deposits of Chignecto Bay (Amos and Zaitlin, 1985). A synthesis of these changes is shown in Figure 3. It appears that Chignecto Bay was under the influence of glacial ice (the Chignecto Phase) prior to 13,300 BP (Scott and Medioli, 1980; Rampton *et al.*, 1984). Submergence of Chignecto Bay through ice loading was greatest (55 m) at approximately 15,000 BP (Quinlan and Beaumont, 1982). Sandy deltas were formed extensively along the front of the retreating Chignecto ice sheet through meltout (Wightman and Cooke, 1978) into the inundated Bay of Fundy (the De Geer Sea, after Lougee, 1953). Concomitant emergence, that took place at a rate of 106 cm/century, elevated the deltas above present sea level (Goldthwait, 1924). Foreset beds of these deltas presently exposed in cliff sections around Chignecto Bay, together with macrofaunal evidence, are diagnostic of microtidal conditions at the time (Grant, 1970; Wagner, 1980). Marine reworking and erosion of glacial deposits into gravel beds subsequent to deglaciation (13,300 to 10,000 BP) is suggestive of strong tidal currents. This is tentatively correlated with

Table 1. A summary of the general dimensions of the Chignecto Bay system

	Shepody Bay	Cumberland Basin	Chignecto Bay
Length of coastline (km)	94.0	68.6	106.7
Littoral area (km <sup>2</sup> )	99	83	46
Sublittoral area (km <sup>2</sup> )	76	38	469
Spring tidal prism (km <sup>3</sup> )	1.43	0.90	5.56
Neap tidal prism (km <sup>3</sup> )	0.91	0.57	3.54

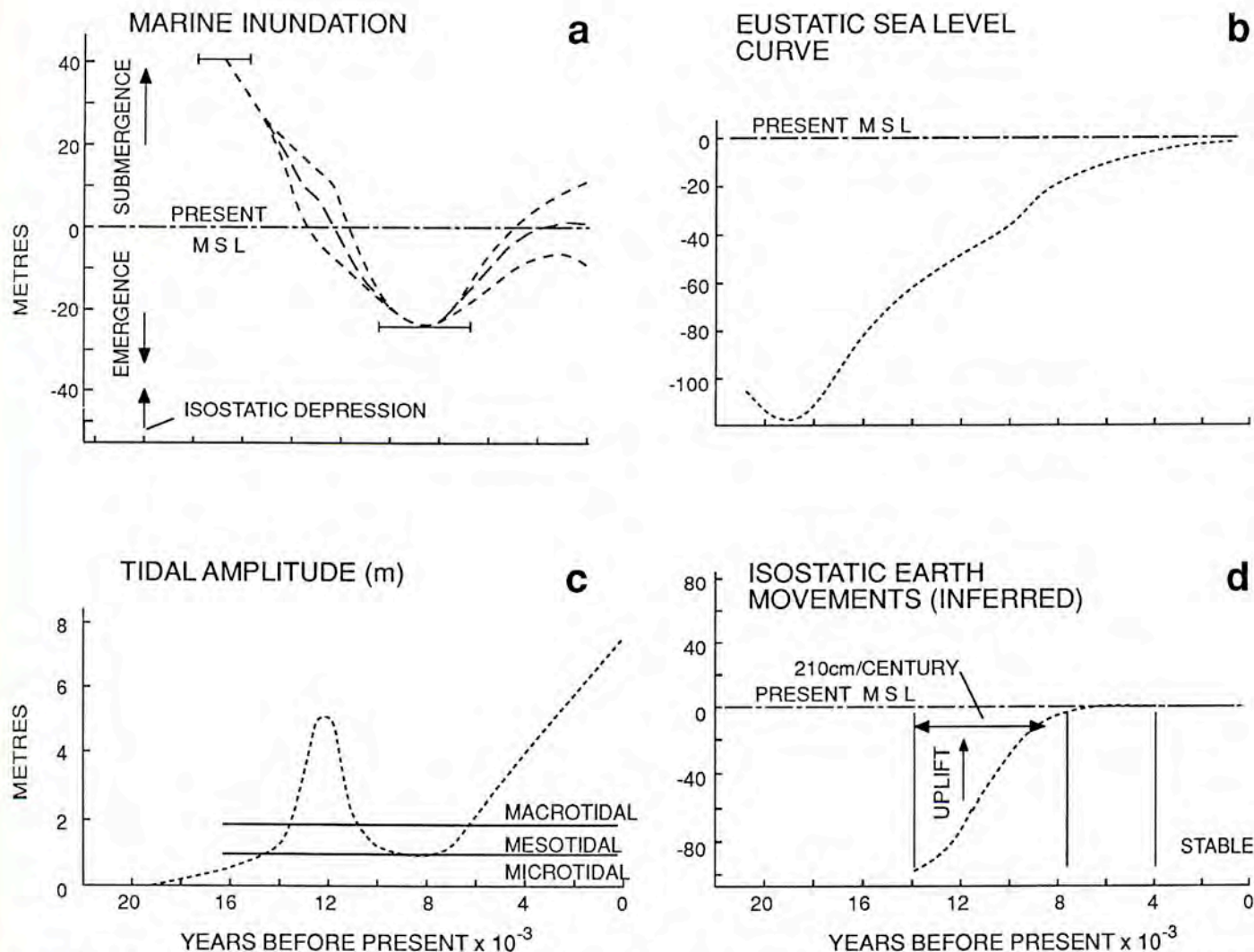


**Figure 3.** A schematic representation of marine inundation of Chignecto Bay over the last 20,000 years. The figure shows: **a.** the position of high water relative to present-day mean sea-level; **b.** a generalized eustatic sea level curve for eastern North America (after Curry, 1960); **c.** the amplitude of the Bay of Fundy tides (after Amos and Zaitlin, 1985); and **d.** the inferred isostatic movements derived by subtracting **a** and **b**.

a brief period of macrotidal conditions that peaked 12,000 BP as postglacial emergence caused sea level to approach that of today (Fig. 3A, C). The uplift rate, derived by summing the eustatic sea level curve of Milliman and Emery (1968; Fig. 3B) and the relative emergence curve (Fig. 3A), was approximately 2 m/century during this time. This rate is comparable with uplift rates during early deglaciation in the eastern Canadian Arctic (Stravers and Syvitski, *in press*).

Fresh water Holocene deposits found at a depth of 25 m below mean sea level at the mouth of Cumberland Basin demonstrate that glacial rebound resulted in the relative emergence of the Chignecto Bay system at least to this depth (note that the Holocene lowstand is corrected from 32 m below sea level reported by Amos and Zaitlin, 1985). This emergence is dated circa 7,000 BP (Quinlan and Beaumont, 1982; Grant, 1985; Amos and Zaitlin, 1985). During this time, Shepody Bay and Cumberland Basin were fluvial valleys and Chignecto Bay was the site of accumulation of estuarine, fine grained deposits (Amos and Zaitlin, 1985) Results of numer-

ical simulations of the Chignecto Bay paleotides by Scott and Greenberg (1983) indicate that the tidal range 7,000 BP was between 1.6 and 2.0 m; that is, microtidal. Subsequently, mean sea level rose at a steady rate of 15 cm/century to its present level with an associated steady increase in tidal range of 30 cm/century (Harrison and Lyon, 1963; Grant, 1970; Scott and Greenberg, 1983). No evidence for isostatic earth movements are evident from 8,000 BP to present. Approximately 20 m of fine grained, "lagoonal" muds were deposited in the sub-estuaries during the Holocene transgression. These muds covered a basal forest horizon described by Chalmers (1894) and mapped by Noordijk and Pronk (1981) under much of the inner estuary.

PAST SEDIMENTARY CHARACTER

The majority of the unconsolidated sedimentary sequence of Chignecto Bay is preserved in the sublittoral, outer part of this estuary. Here, a sequence over 50 m thick has infilled a meandering, steep-sided paleochannel that runs

along the median line of the system (Fig. 4). The sequence comprises five seismo-stratigraphic units (G1 to G4 and R) separated by four acoustic discontinuities (Fig. 5). These units are correlated with lithological and stratigraphic attrib-

utes from nineteen vibracores analyzed by Amos and Zaitlin (1985; Figs. 6, 7). The stratigraphic units consist of ten distinct lithofacies:

*Facies M* (clayey mud) — massive to indistinctly laminated

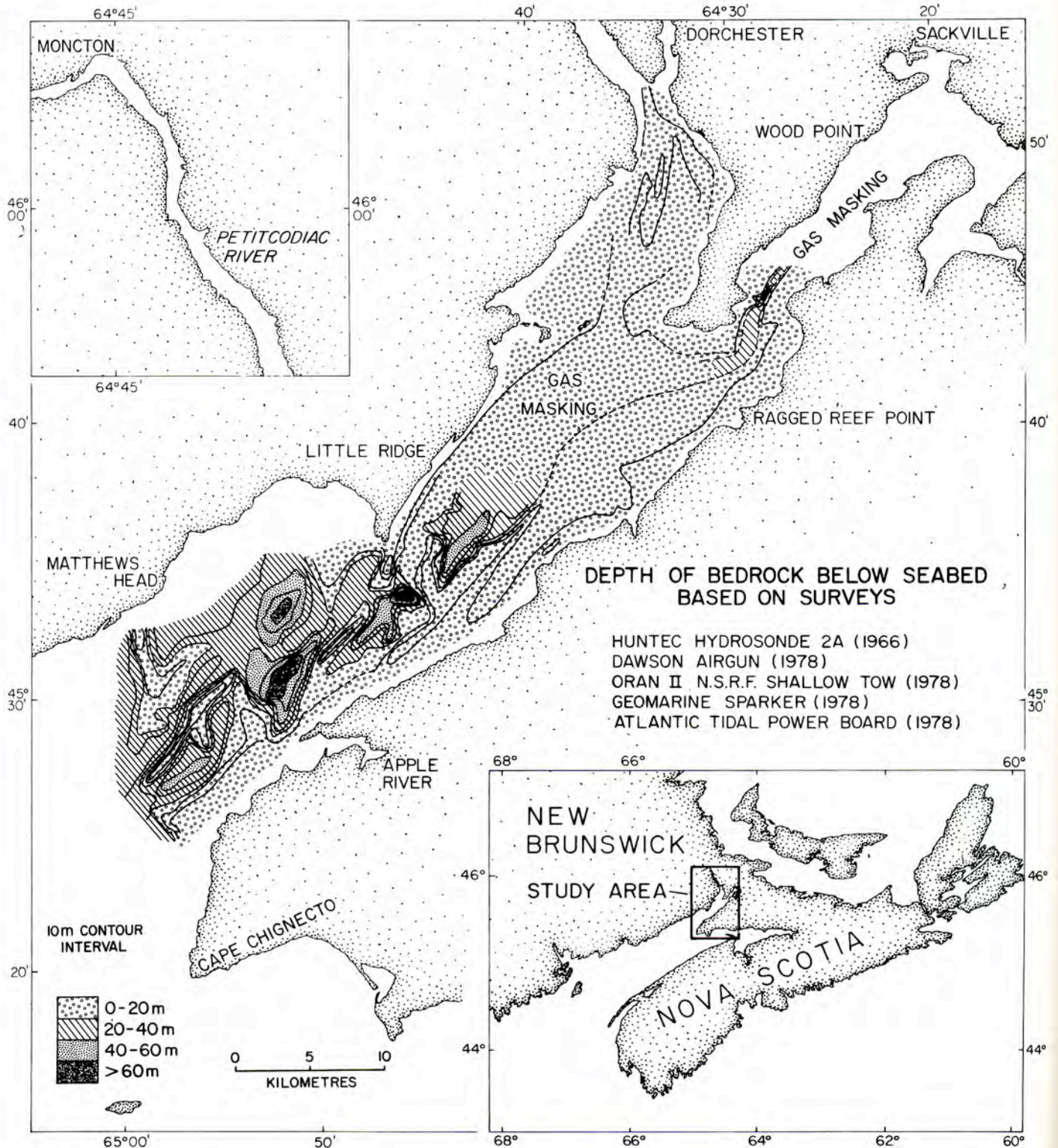


Figure 4. An isopach map of the surficial sediments of Chignecto Bay. The greatest thickness of sediments occurs in the buried channel system of the outer bay. Acoustic masking due to the presence of gas in surficial sediments prevents detailed mapping in the inner bay. Barriers across the estuary are evident off Matthews Head and Little Ridge. These barriers are composed of well-rounded sand and gravel from unit G3.

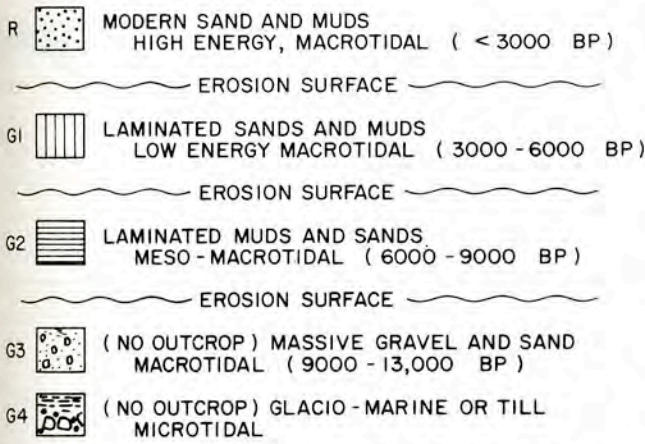


Figure 5. Generalized stratigraphy of the surficial sediments of Chignecto Bay, based on analyses of vibracore samples and seismic records. G4 is glacial in origin, G1 to G3 are postglacial estuarine deposits, and R is Recent (less than 3,000 years old).

red clay to silty/clayey mud (Fig. 8, core 3), ranging in thickness from 10 mm to 2 m. It is characterized by horizontal and vertical burrows and the presence of marine bivalve fragments.

*Facies M<sub>p</sub>* (pebbly clayey mud) — massive to weakly laminated, red clayey mud with 10 to 30 per cent well-rounded pebbles or small cobbles in a poorly sorted matrix.

*Facies M<sub>b</sub>* (bioturbated pebbly clayey mud) — similar to facies M<sub>p</sub> but a high degree of bioturbation is evident (Fig. 9, core 13).

*Facies L* (lenticular-bedded sandy mud) — massive to well-laminated, bioturbated, red clayey mud (facies M) occupying 60 to 85 per cent of the unit, interbedded with rippled silts or fine sands (Fig. 8, core 10; Fig. 10, core 11). Sands have distinct erosional bases, well-defined tops and form pods or lenses 10 to 30 mm thick. Medium-to high-angle planar and trough crosslaminae are evident in the sands.

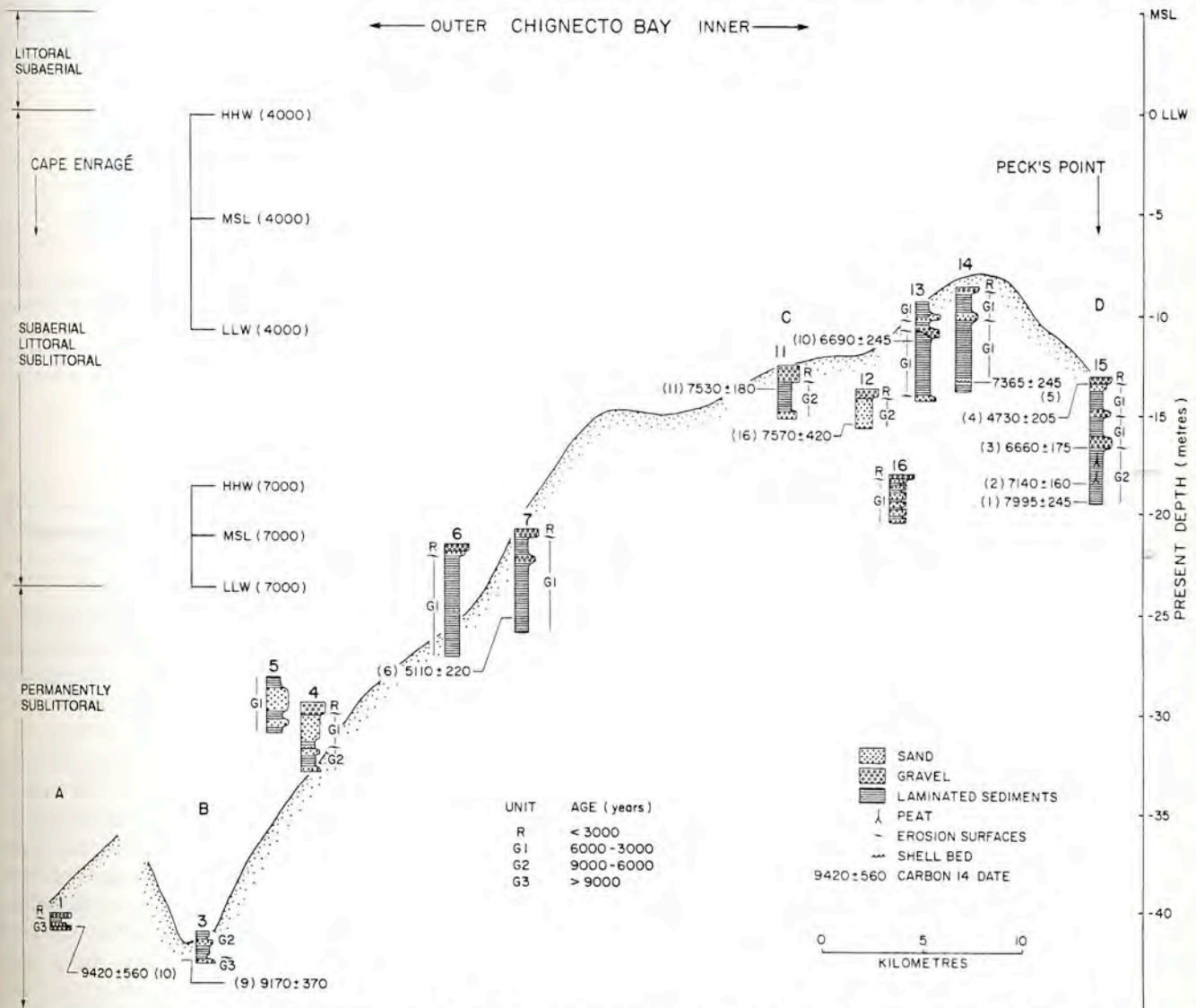
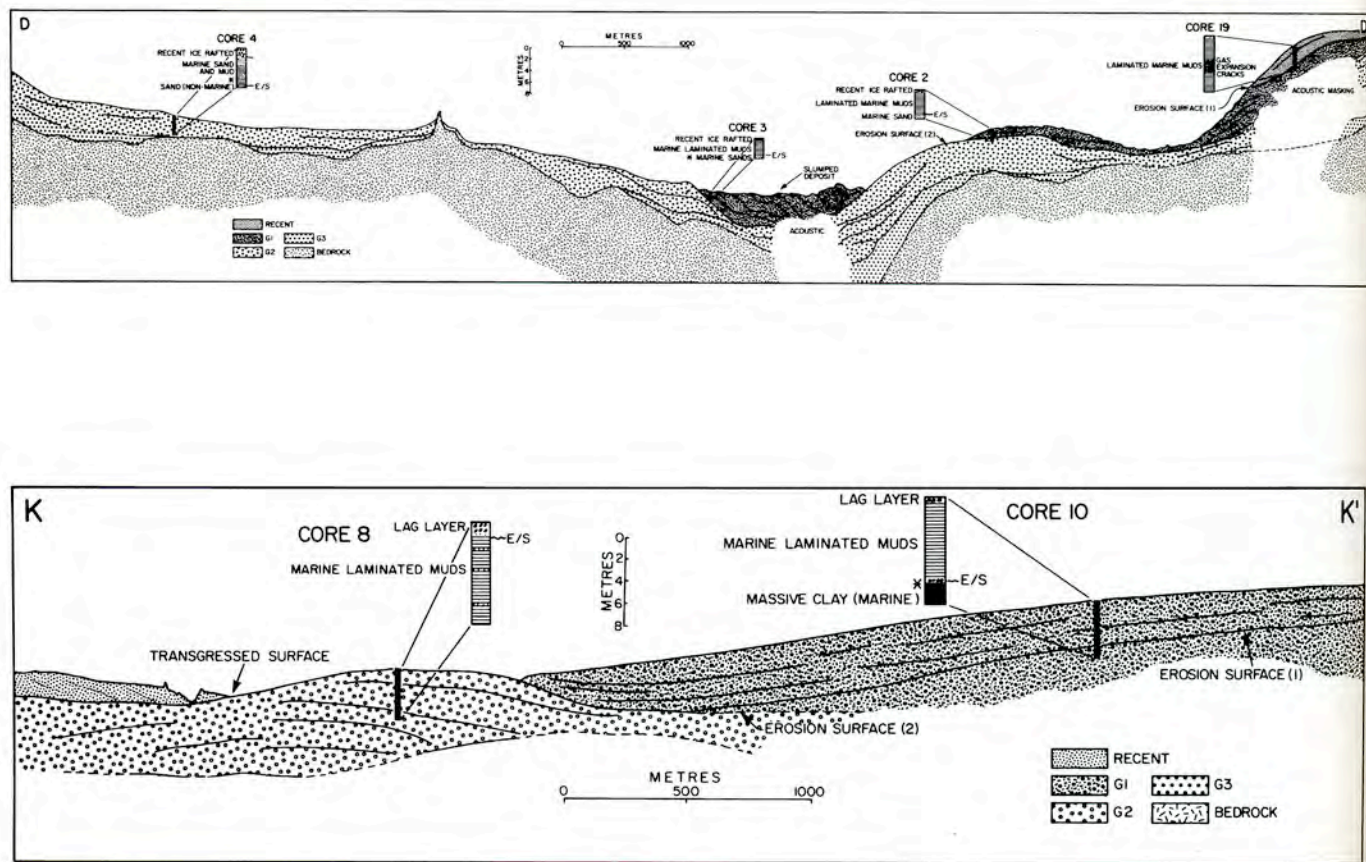


Figure 6. The generalized lithology and relative position of 12 vibracores collected along a median section of Chignecto Bay (after Amos and Zaitlin, 1985). The positions of highest high water (HHW), mean sea level (MSL) and lowest low water (LLW) 7,000 and 4,000 BP are shown for comparative purposes. A complex pattern of littoral and sublittoral settings has evolved, modified by drastic changes in tidal range.



**Figure 7.** Two interpreted seismic sections through Chignecto Bay illustrating the seismo-stratigraphic units of Figure 5. The gross lithology measured from vibracores collected along the sections is also shown. D-D' is an east-west section near Cape Enragé (see Figure 13 for location) showing the central buried channel infilled with slumped deposits of unit G1 (3,000 to 6,000 BP). Erosion surfaces 1 and 2 are also visible in the section. Note that the present-day surface is covered by a thin veneer of gravelly sediment interpreted as a winnowed lag. Section K-K' is a northeast-southwest section off Cape Maringouin showing a good correlation between acoustic reflectors and sand beds within vibracores 8 and 10. The predominance of G1 and G2 is evident in the section as is the transgression surface that bounds them.

*Facies W* (wavy-bedded muddy sand) — wavy-bedded silt or medium sand, interbedded or interlaminated with facies M (Fig. 11, core 9). Sands have sharp, erosional bases and undulatory tops. Planar and trough crosslaminae occur in the sand, cut by low angle reactivation surfaces. Bioturbation is restricted to facies M.

*Facies F* (flaser-bedded muddy sand) — silty, very fine to medium rippled sand (60-85%) interlaminated with lenses of facies M (Fig. 11, core 5). The muds predominate in the troughs of the rippled sand and are bioturbated.

*Facies S<sub>c</sub>* (coarse grained sand) — massive, medium to coarse grained sand forming laminae and beds 10 mm to 0.2 m in thickness (Fig. 11, cores 5, 9; Fig. 10, cores 7, 3). A distinct depositional cycle is evident in this unit, starting with an eroded base that is overlain by a fining-upward sequence of shelly sand.

*Facies S<sub>p</sub>* (pebbly sand) — massive to poorly bedded granules or coarse sand beds up to 0.2 m thick, bearing pebble inclusions (15-25%; Fig. 8, core 3). The base of the sand is distinctly eroded and has 20 mm of relief. The unit fines upward into facies M, L or F.

*Facies G* (gravel) — massively bedded, well rounded pebbles of moderate sorting. A matrix of shelly sand forms 20 to 40 per cent of the facies (Fig. 10, core 3). It has an abrupt upper contact and is overlain by facies M or L.

*Facies P* (peat) — The base of the unit is characterized by rooted, grey-green, silty seatearth. It is overlain by laminated, grey-green to dark grey mud, containing roots in growth position (Fig. 12, core 15). This facies is associated with fresh water microfauna (A. Miller, pers. comm., 1986).

The seismo-stratigraphic sequence interpreted from acoustic data is shown in Figure 13. The base of the sequence is interpreted as being characterized by glaciomarine sediments or till deposited during the Chignecto Phase (acoustic unit G4). It is found only in the deeper parts of the bay infilling irregularities in the underlying bedrock surface (seen on original Huntect Hydronsonde 2A records of Swift *et al.*, 1973). This unit is up to 5 m thick. It is not known to outcrop in the bay.

The oldest marine deposits (acoustic unit G3) sampled were in cores 1 and 3 (Figs. 6, 8, 10). This unit is up to 30 m thick and generally rests on bedrock (Fig. 7, section D-



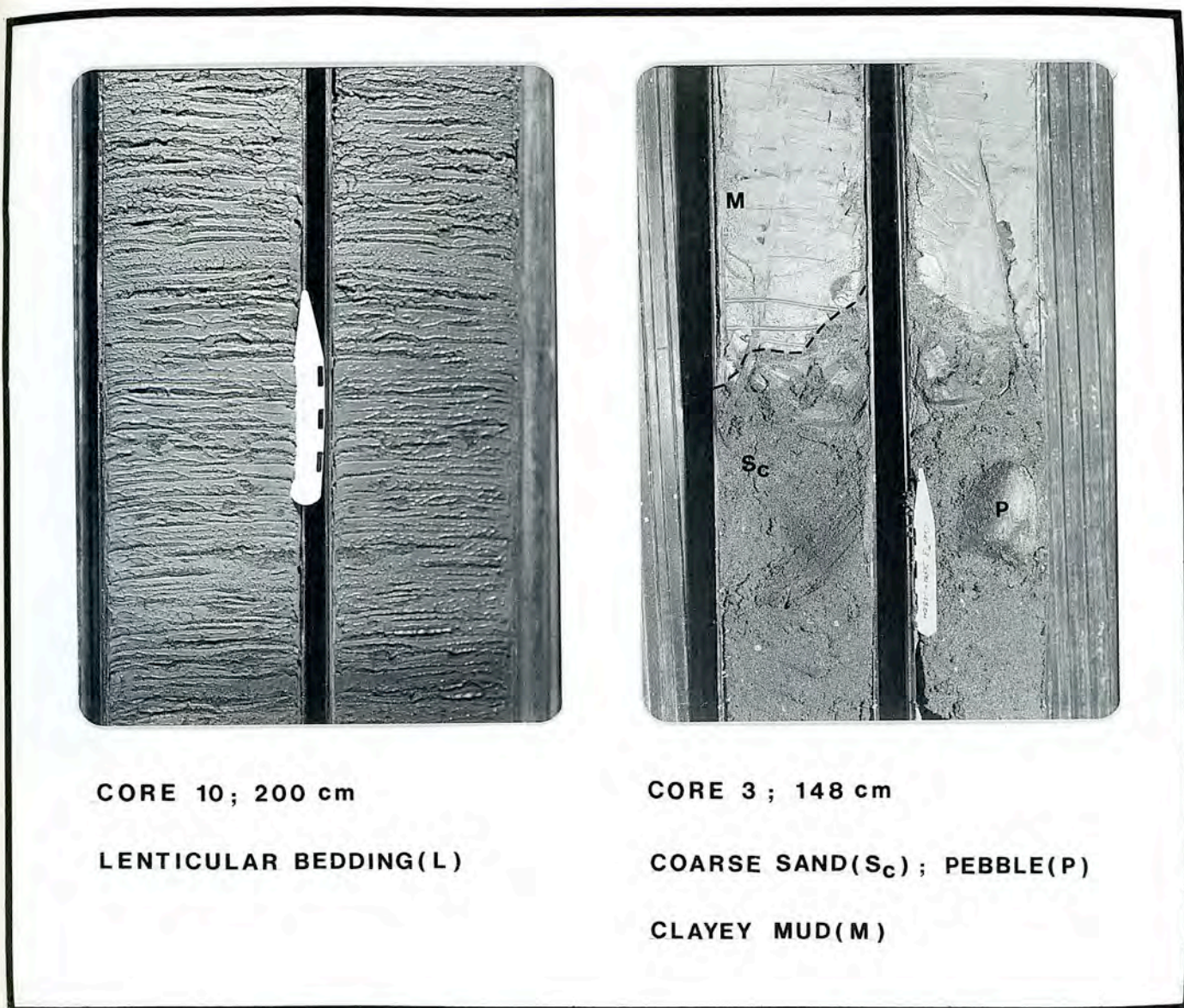


**Figure 8.** Core 10: lenticular bedding (L) at a depth of 2.00 m in unit G1 (see Fig. 7; section K-K'). Note the rhythmic bedding, the dominance of mud and the lack of any obvious cyclicity in laminae thickness. Core 3: the erosion surface separating units G1 (the clayey-mud facies, M) and G2 (the coarse sand facies, S<sub>c</sub>; see Fig. 7). The irregular erosion surface is the result of G1 have slumped over G2 (section D-D'). The coarse facies is interpreted as representing a brief period of macrotidal activity approximately 9,000 BP. The scale in each plate is graduated in cm and the scale point indicates the top of the sequence.

D'). Sediments are composed of facies G, S<sub>p</sub> and S<sub>c</sub>, which were deposited approximately 9,000 to 13,300 BP within a sublittoral setting. A marine origin for the unit is evident by the presence of the macrofossils *Spisula* sp. and *Mytilus edulis* (Table 2). The system at that time was regressive. The lower part of the unit formed, therefore, at a depth no greater than 50 m below extant sea level. The dominance of well-rounded gravel in this unit is attributed to currents associated with a brief period of high-energy macrotidal conditions as sea level passed through sea level today (12,000 BP). The Chignecto Bay system during late Pleistocene was likely con-

nected to the Gulf of St. Lawrence. It is proposed that the isthmus of Chignecto (that joins New Brunswick and Nova Scotia; see Fig. 2) emerged during this period of regression, thus isolating the Bay of Fundy from the Gulf of St. Lawrence and providing a suitable bay geometry for macrotidal conditions.

The upper part of unit G3 was deposited in a littoral setting in the form of a barrier at the mouth of the paleoestuary (Plate 3, core 1, C-14 dated at 9,420 BP in Amos and Zaitlin, 1985). The barrier developed at the paleoestuary mouth as sea level fell 20 m below that of today during late



CORE 8 ; 400 cm

LENTICULAR BEDDING ( L )

BIOTURBATION ( b )



CORE 13 ; 490 cm

COARSE SAND ( S<sub>c</sub> ) ; MUD ( M )

FLASER BEDDING ( F )

**Figure 9.** Core 8: highly bioturbated, lenticular bedding from the mesotidal deposits of unit G2 (Fig. 7, section K-K'). Core 13: highly bioturbated muds, flaser deposits and massive coarse sands from the macrotidal deposits of unit G1.

G3 time. We postulate that wave conditions at the time were able to create this barrier through reworking of underlying glacial debris in a fashion similar to cobble barriers across the mouth of estuaries on the Gulf of St. Lawrence (Syvitski *et al.*, 1987) and across fjords of Baffin Island (Taylor *et al.*, 1987).

Unit G2 overlies unit G3 and is separated from it by a widespread acoustic discontinuity that correlates with an eroded surface (Fig. 8, core 3). It was deposited between 9,000 and 6,000 BP. It is up to 10 m thick and underlies most of Chignecto Bay, outcropping in the eastern and extreme western parts of the bay (Fig. 13). It is thickest along the eastern margin of the central estuary. Off Cape Enragé it is highly variable in thickness, varying in an estuary-parallel

pattern. It is dominated by a stiff, dry, muddy facies M (41%), L (39%), and P (7%) with only minor amounts of facies W, S<sub>c</sub>, S<sub>p</sub> and M<sub>p</sub>. Massive muds predominate in the lower part of the sequence whereas fine (approximately 10 laminae per cm), lenticular laminae dominate the upper part. The change in facies is interpreted as a result of a decrease in water depth as G2 was deposited. There is an abundance of organic detritus and a distinct, well-preserved macrofauna uniquely characterized by the gastropods *Acteocina canaliculata* and *Crepidula fornicata* (Table 2). These fauna are diagnostic of shallow marine conditions subject to a fluctuating salinity. Facies L are intercalated with fresh water peats and salt marsh deposits (facies P) at the mouth of Cumberland Basin and are, therefore, littoral in origin (see

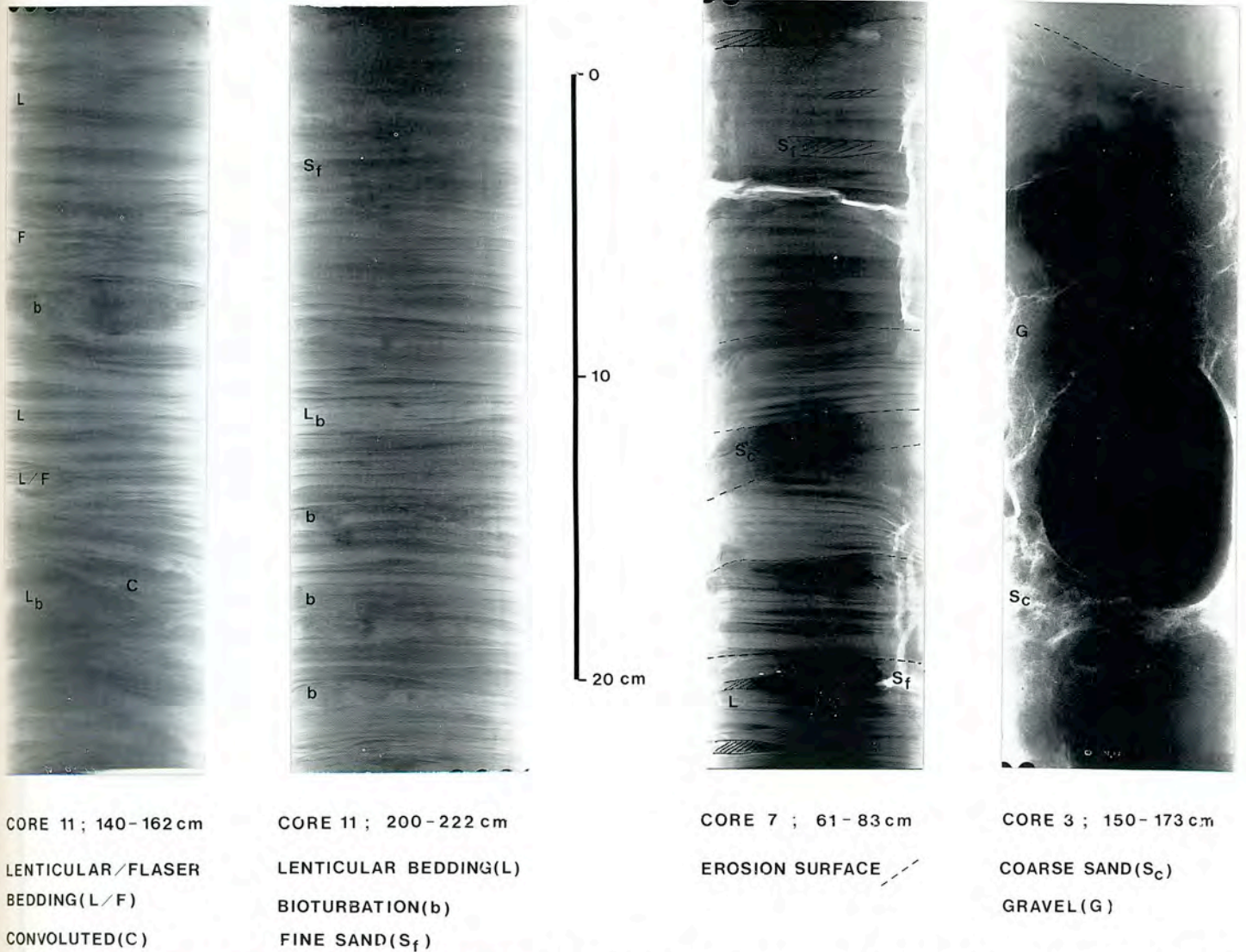


**Figure 10.** Four positive X-radiographs of vibracore samples. Core 11: lenticular bedding with evidence of bioturbation from unit G2. Core 7: laminated sand/fines from unit G1. Note the interbedded, tabular, ripple crosslaminated fine sand and the abundance of erosion surfaces. Core 3: well-sorted coarse sand interspersed with well-rounded pebbles and cobbles. The dashed line denotes the boundary between G3 (below) and G2 (above).

Figs. 6, 12, core 15). This interpretation is supported by the seismic character of the unit. The seismic section in Figure 7 (K - K') shows convex up, gently-dipping reflectors diagnostic of point bar lateral accretion beds associated with littoral creek migration (Nio and Yang, 1989). Dewatering structures (seen in core 11) are typical of present-day creeks in the Bay of Fundy that have developed in regions of high deposition.

The final stages of deposition of unit G2 coincided with a mid-Holocene lowstand in sea level (Fig. 3A). Microtidal to mesotidal conditions are interpreted to have prevailed based on the dominance of the fine grained facies. The salt marsh sequence is up to 2.5 m thick and yields a deposition rate of 0.1 mm/year (note that this rate does not account for the effects of sediment compaction). The overall lithofacies distribution of this unit is characterized by a transition

from the dominance of facies M in the southwest to facies L in the central part of the bay, to a cyclic sequence of facies M - L - P in the northeast (Table 3). This sequence of facies is interpreted to represent the transition from a sublittoral zone at the mouth of Chignecto Bay, to a lower tidal flat in central Chignecto Bay, to an upper tidal flat in the region of Cape Maringouin. Shepody Bay and Cumberland Basin were subaerial at this time.

A well defined unit of mesotidal to low energy macrotidal muddy, lenticular, wavy and flaser bedded sands and muds (G1) overlies unit G2 and is separated from it by a widespread erosion surface (Fig. 8, core 10; Fig. 9, cores 8, 13). This unit is up to 12 m thick, and is thickest along the median line of the central estuary. It is characterized by facies L (72%) and F (16%) with minor amounts of facies M, W,  $S_c$  and G (Fig. 10, core 13). There is a significant



CORE 5; 250 cm

FLASER BEDDING (F)

COARSE SAND (S<sub>C</sub>)

CORE 9; 17 cm

WAVY BEDDING (W)

COARSE SAND (S<sub>C</sub>)

**Figure 11.** Core 5: flaser bedding and coarse sand from unit G1, outer Chignecto Bay. The sand shows evidence of planar ripple crosslamination; flaser facies are highly bioturbated. Core 9: coarse sand from unit R overlying abruptly wavy bedding from unit G1. The sand shows evidence of tabular crosslamination; the wavy bedding is highly bioturbated.

increase in the abundance of facies F and L over underlying units, an increase in the abundance of ripple crosslaminated sand and gravel and a decrease in bioturbation. The unit is characterized by a facies transition of L - F - M. Lamina thickness is greater (2-3 laminae per cm) than in G2, indicating higher transport and deposition rates (the mean deposition rate of the unit was 3.3 mm/a). The macrofaunal assemblage is unique though poorly developed. It is characterized by the pelyceps *Ensis directus* and *Thyasira flexuosa* and the gastropods *Oenopota harpularia*, *Lunatia pallida* and *Hydrobia totteni* (Table 2). This assemblage is diagnostic of a salt marsh environment with strong tidal currents. The doublets of sand and mud, common in this unit (Fig. 8, core 10; Fig. 10, core 7) are diagnostic of point bar lateral accretion under a tidally varying current (Nio and

Yang, 1989). The convex-up attitude of the acoustic reflectors and the presence of low angle cut-and-fill structures indicate that the majority of this unit was reworked by creek migration. Thin beds of fine grained sand show tabular crosslamination diagnostic of straight-crested ripple migration. No herringbone crosslamination was seen; all cross-sets are oriented in the same direction.

The sediments of this unit are fully saturated and very soft, suggesting rapid deposition. The unit shows evidence of sediment deformation and massive slumping into the central channel (Fig. 7, D-D'). The slump illustrated in Figure 13 is 6 km long and up to 1 km wide and flowed down a slope of 1:100. The unit is dated to have been deposited between 3,000 and 6,000 BP and is, therefore, a transgressive deposit (see Fig. 3A). It occurs principally in inner Chignecto

Table 2. Macrofossil assemblage — Chignecto Bay.

MACROFOSSIL		0 - 3000	3000 - 6000	6000 - 9000	> 9000
<i>Hiatella arctica</i>	p	x			
<i>Nucula proxima</i>	p	x	x		
<i>Yoldia limatula</i>	p	x	x		
<i>Yoldia myalis</i>	p	x	x		
<i>Ensis directus</i>	p		x		
<i>Thyasira flexuosa</i>	p		x		
<i>Oenopata harpularia</i>	g		x		
<i>Lunatia pallida</i>	g		x		
<i>Hydrobia totteni</i>	g		x		
<i>Mya arenaria</i>	p		x	x	
<i>Retusa obtusa</i>	g		x	x	
<i>Crepidula fornicata</i>	g		x	x	
<i>Nassarius trivittatus</i>	g	x	x	x	
<i>Mitrella lunata</i>	p	x	x	x	
<i>Cerastoderma pinnulatum</i>	p	x		x	
<i>Mulinia lateralis</i>	p	x		x	
<i>Macoma balthica</i>	p	x		x	
<i>Acteocina canaliculata</i>	g			x	
<i>Crepidula fornicata</i>	g			x	
<i>Spisula polynyna</i>	p				x
<i>Mytilus edulis</i>	p	x	x	x	x

Bay, and along the axes of Shepody Bay and Cumberland Basin; that is, in the inner part of the paleostuary. The lower part of the deposit was formed in a littoral, low energy (4-6 m tidal range) macrotidal setting, whereas the upper part was deposited in a sublittoral, medium energy (6-8 m tidal range) setting in the central part of the paleoestuary. The unit outcrops in the eastern-central part of Chignecto Bay and along the central parts of Shepody Bay and Cumberland Basin (Fig. 13).

Modern, high energy (8-12 m tidal range), macrotidal sand and gravel deposits are being created under present-day tidal conditions (R). These sands are dominated by the

Table 3. The major facies cycles recognized in each of the four sampled seismo-stratigraphic units. G3 and R are dominated by sand and gravel facies (diagnostic of intense reworking) whereas units G1 and G2 are dominated by muddy facies (diagnostic of a dominantly depositional environment).

## Major Cycles

G3	G
G2	M - L - P
G1	L - F - M
R	Sp - Mpb - Sc



CORE 15 ; 480 cm

SALT MARSH ( sm )

ROOTLETS ( R )

Figure 12. Core 15: salt marsh rootlets in growth position from a massive clay facies at a depth of 4.80 m below the seabed at the mouth of Cumberland Basin. The sample comes from unit G2 and formed approximately 7,000 BP.

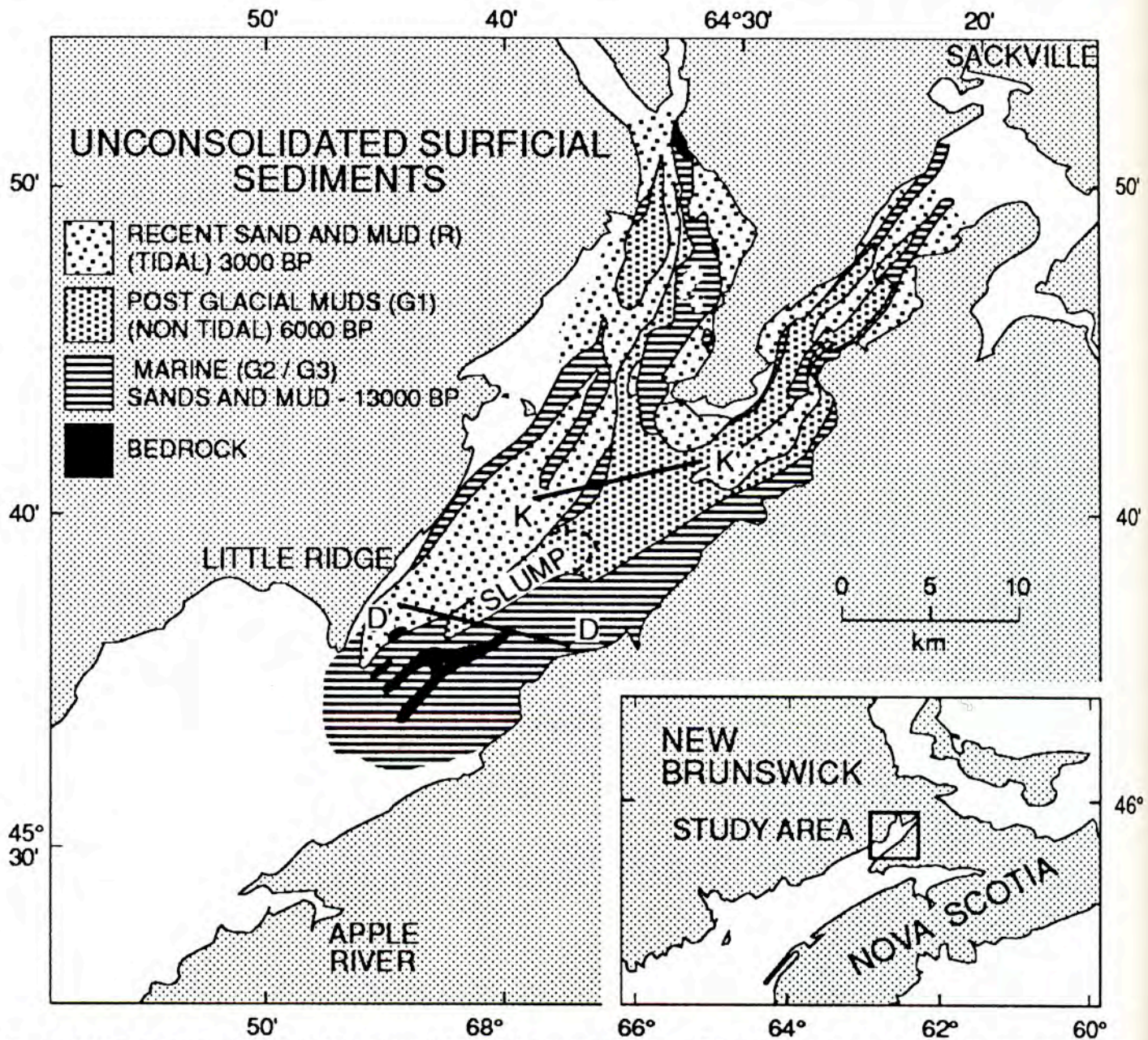


**Figure 13.** A seismo-stratigraphic map of the unconsolidated sedimentary sequence in Chignecto Bay illustrating the major acoustic units. Note the zone of slumped sediments, illustrated in section D-D' (Fig. 7). This slump is 6 km in width and approximately 1 km long. The origin of the slump is unknown.

facies  $S_c$ ,  $S_n$  and  $M_{pb}$  and are uniquely characterized by the pelycepod *Hiatella arctica*. Such conditions we consider to have prevailed for approximately 3,000 years. Much of this deposit is reworked from the underlying sequence and is separated from it by a well developed, transgressed, eroded surface (Fig. 7; K-K', core 8). Sublittoral sandy equivalents form an asymmetrical wedge that thins headward and to the west. It is thickest (2 m) along the extreme eastern portion of the central estuary. No sublittoral, fine grained deposits are known to be presently forming in the Chignecto Bay system. The mud facies of this unit were deposited in the present-day littoral parts of the system in a manner reviewed by Dalrymple *et al.*, (*this volume*).

#### MODERN HYDRODYNAMIC PROCESSES

##### TIDES

The tidal regime of Chignecto Bay is dominated by the lunar semidiurnal component because of its near-resonance with the Gulf of Maine/Bay of Fundy system (Garrett, 1972). The amplitudes of the diurnal  $K_1$  and semidiurnal  $M_2$  components are 0.15 and 4 m, respectively, illustrating the small diurnal contribution to tidal range. Similarly, the amplitude ratios of the  $N_2/M_2$  and  $S_2/M_2$  are about 0.22 and 0.16, respectively. The amplitude of the  $M_2$  tide in Chignecto Bay increases from 4.2 m at the mouth to 4.4 m off Cape Enragé to 4.7 m at the mouths of Cumberland Basin and

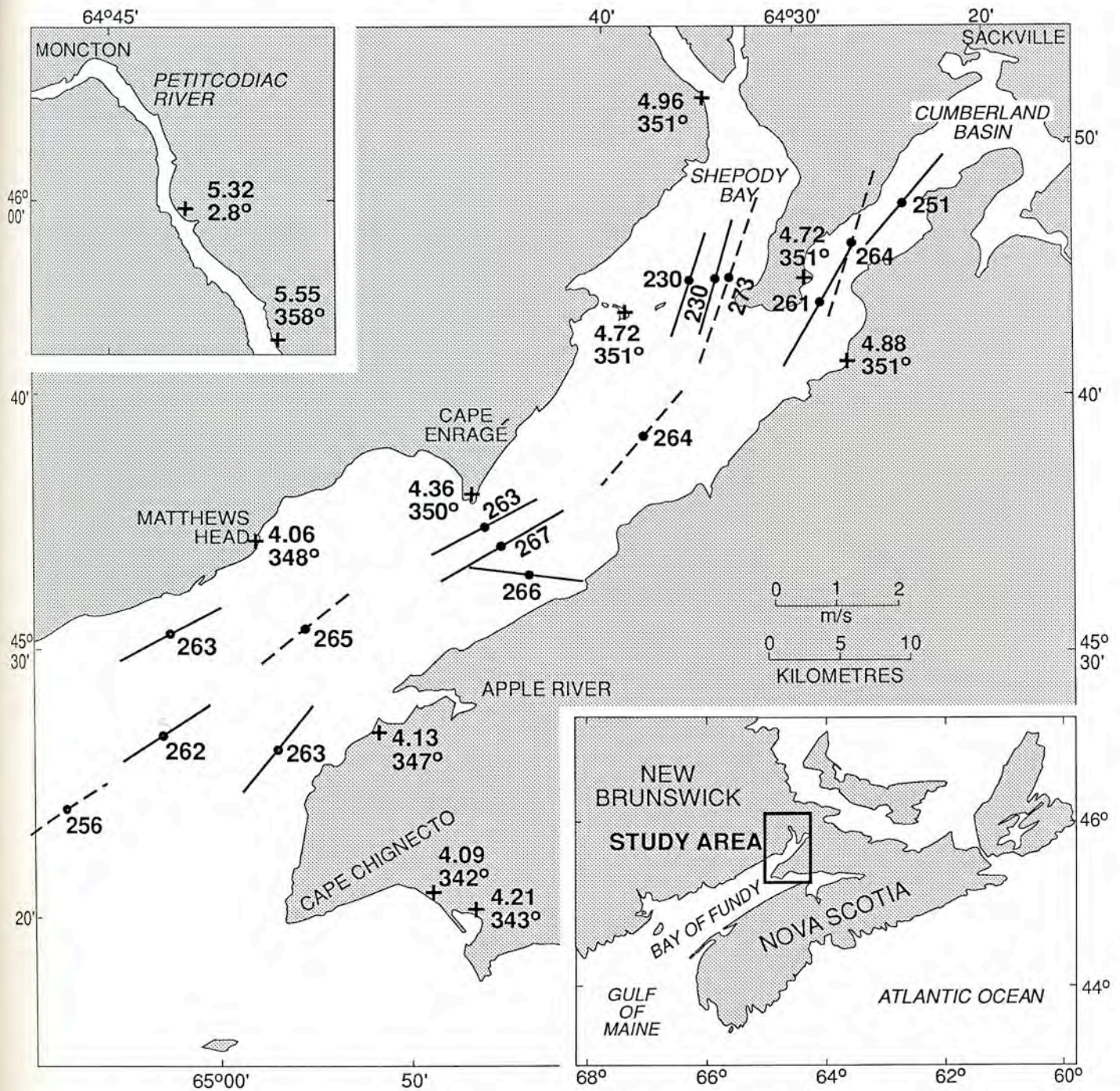


**Figure 14.** The major and minor axes of the observed tidal ellipses in Chignecto Bay. The data collected during this study are shown by solid lines. Data collected by Godin (1968) are illustrated as dashed lines. The numbers near the axes refer to station number. Peak currents vary between 1 and 2 m/s and generally parallel the estuary margins.

Shepody Bay (Godin, 1980; deMargerie and Dewolfe, 1987; Greenberg, pers. comm., 1990). The respective Greenwich phase lags systematically from 347° to 350° and 351°. This corresponds to a variation in the times of high and low water of 8.3 minutes. The neap-spring oscillation is 0.38 times the  $M_2$  amplitude. The diurnal inequality ( $M_2/M_2$ ) in tidal amplitude is about 0.02 at the mouth of Chignecto Bay, 0.03 at the mouths of Shepody Bay and Cumberland Basin, and

0.09 near the head of the system. This is very small compared to values reported for Dutch mesotidal estuaries (Nio and Yang, *this volume*).

**CURRENTS**

*Tidal Currents*

The currents of the semidiurnal  $M_2$  constituent dominate flow patterns in the Chignecto Bay system. The

major and minor axes of the  $M_2$  tidal ellipses are shown in Fig. 14 (solid lines). The figure also shows the results of the 1965 survey carried out by Godin (1968; stations 66-71; dashed lines). The depth-averaged semi-major axes of these ellipses increase from between 0.7 to 0.8 m/s near the mouth of the system to between 1.0 and 1.5 m/s at the mouths of Cumberland Basin and Shepody Bay and are greater than 1.5 m/s in the tidal channels at the estuary head. Currents are generally parallel to the channel margins in which they flow. The tidal ellipses are virtually rectilinear, with the semi-minor axes usually an order of magnitude smaller than the semi-major axes. Rotation of the current ellipses is mainly anticlockwise. The Greenwich phase lag of the semi-major axes varies between  $260^\circ$  and  $270^\circ$  and leads the tidal elevation by approximately  $90^\circ$  (Fig. 15C). Near-surface currents at the mouths of Shepody Bay and Cumberland Basin (stations 70-71) were considerably larger than near-bed ones (stations 291, 303, 304) and were consistent with short-term observations made at nearby anchor stations.

Examination of measurements of the current flow at the mouth of Chignecto Bay, made by Tee (1982; stations 283, 284, 306), showed that the semi-major axes decreased from surface to bottom. He found a typical ratio of near-bed to mid-depth currents to be between 0.65 and 0.75. Also, he found the phase lag to decrease toward the seabed between  $5^\circ$  and  $10^\circ$  with a change in rotation of the semi-minor axes from clockwise (negative) near the surface to anticlockwise (positive) near the seabed. By contrast, the orientation of the semi-major axes changed only slightly with depth.

### Residual Currents

The residual current is the time-average mean of measures of speed and direction over a period long enough to eliminate tidal and storm-driven signals. Figure 16 shows the residual current so calculated from measurements in Chignecto Bay. Notice that the greater part of these residual currents, in contrast to the tidal currents, are oriented across the bay, not parallel to its margins. The maximum and minimum residual currents both exhibit this pattern. Minima approach zero at mid-depths near the mouth of the system (Fig. 14, stations 283, 284, 306). Maxima approach a velocity of 0.17 m/s and occur near Cape Enragé. Here, the residual current direction is to the southeast. This trend results from the presence of two, tidally-induced residual gyres; a clockwise gyre southwest of Cape Enragé and an anticlockwise gyre to the northeast (Greenberg, 1983; Tee and Amos, *in press*).

Residual current directions in Cumberland Basin (Fig. 9, stations 70, 290) are to the east and northeast, while nearer the mouth (station 291) they flow westward. The along-channel component of the residual current is upstream near the surface and downstream near the bed. This pattern does not conform with the classic Pritchard (1956) estuarine circulation model. Here, the residual currents are unlikely to be a result of water density variations. Rather they appear to result from effects of tidal propagation through complex channel geometry in shallow water.

Residual currents at the entrance to Shepody Bay are to the north and northwest. Observations are consistent with

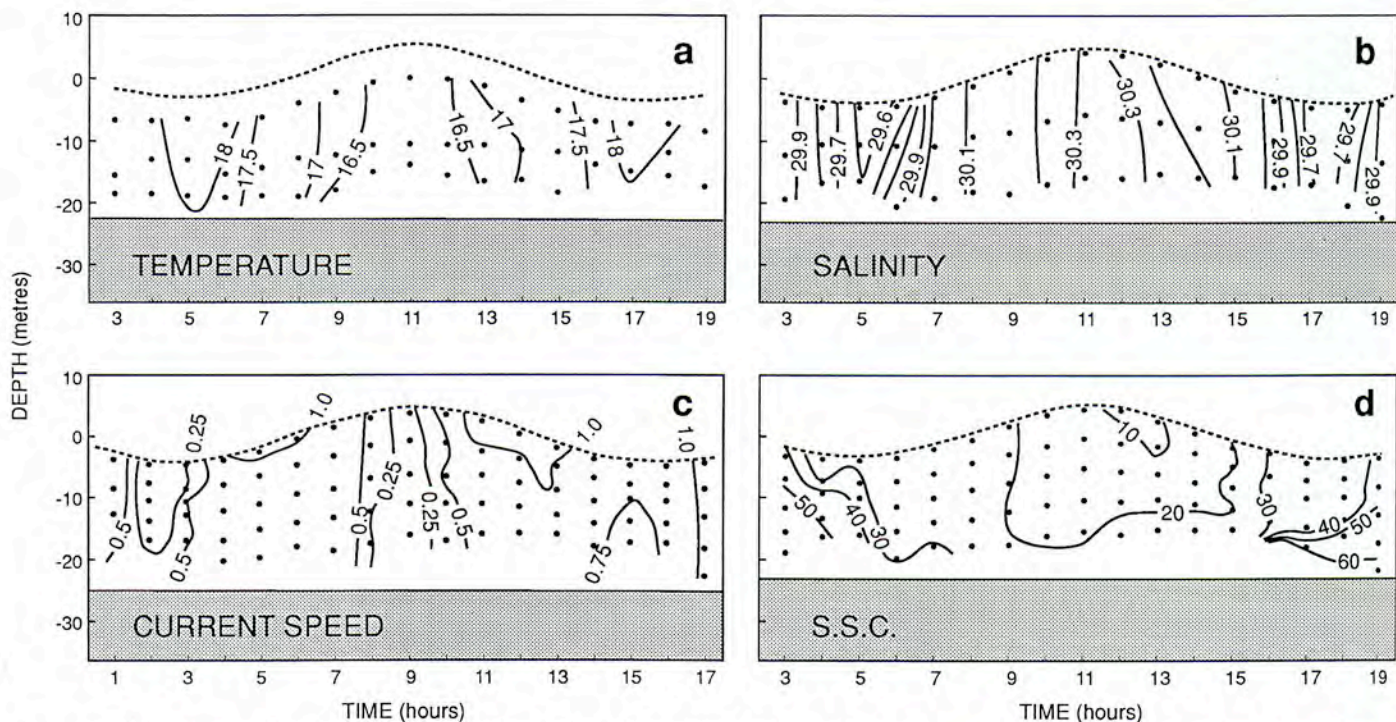


**Figure 15.** Measurements from station 9 (mouth of Shepody Bay, Fig. 2C) collected 8 August, 1978; **a.** temperature; **b.** salinity; **c.** current speed; and **d.** suspended sediment concentration. Observations throughout the water column were made hourly from 1 hour before low water to 1 hour after the successive low water (approximately 15 hours). Note in **d** the near-bed increase in SSC during slack tide, and the absence of stratification in **a** and **b**.



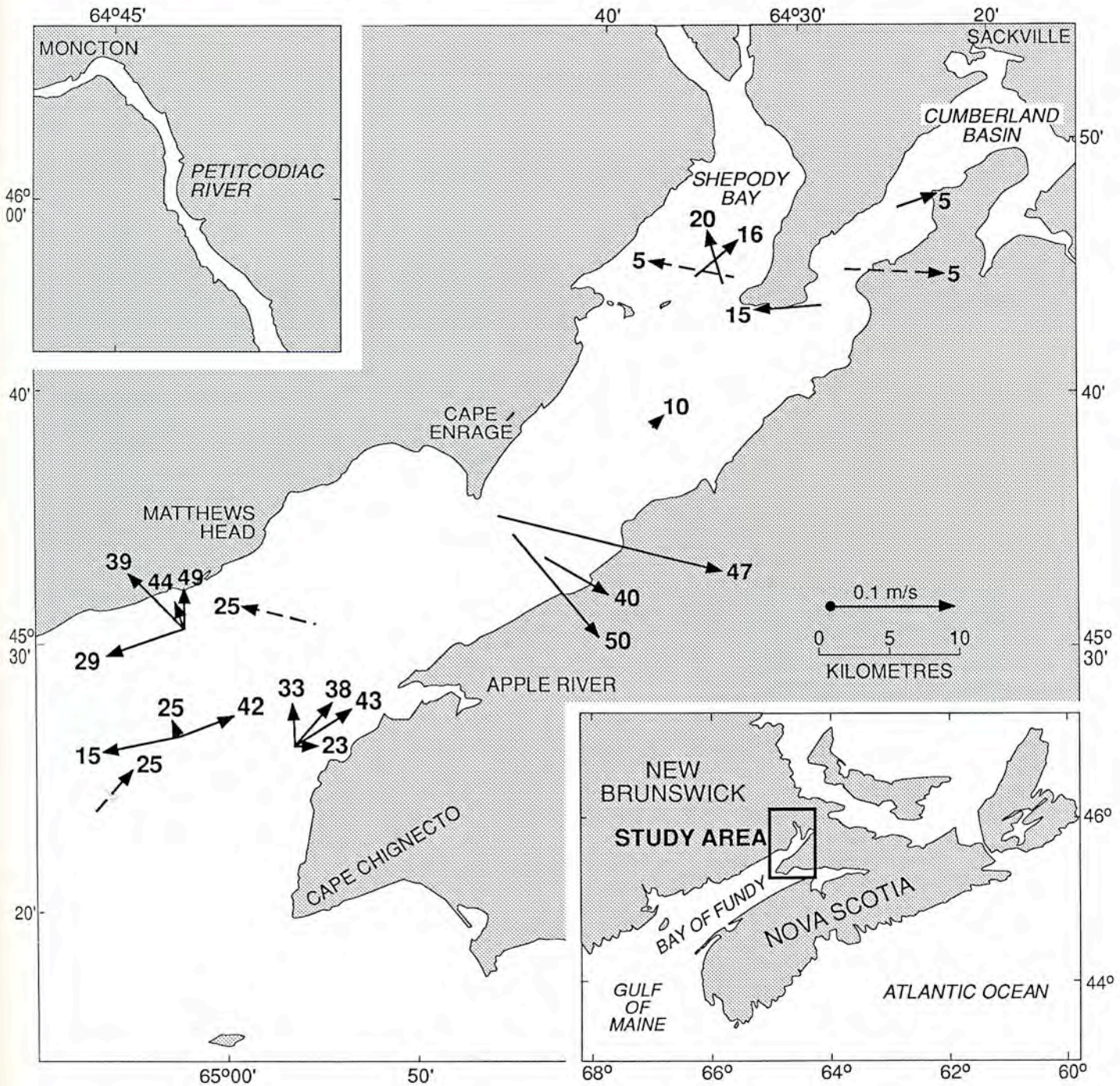


**Figure 16.** The measured residual currents in Chignecto Bay. Data collected during this study are shown as solid arrows; results of Godin (1968) are shown as dashed arrows. Numbers at the arrow heads denote the depth (in m) of the observation. The magnitude of residual currents rarely exceeds 0.15 m/s. Note the peculiar directions of residual flows; the result of gyres in the system.

the tidally-induced residual currents modelled by Greenberg (1983), who showed the existence of an anticlockwise gyre at this site. Measured residual currents at the mouth of Chignecto Bay are oriented in the along-channel direction. Surface measurements indicate a net outflow from the system whereas near-bed measurements indicate an inflow. Outflow is greatest in the western portion; inflow is greatest to the

east. This pattern is likely a result of horizontal gradients in density.

**WAVES**

The entire Chignecto Bay system is influenced by winds blowing up the Bay of Fundy from the southwest. These winds are responsible for the generation of locally-generated

**Table 4:** The measured wave climate recorded at Cape Maringouin and Cape Enragé between June, 1978 and February, 1979 (from Marine Environmental Data Service, 1979(a) and 1979(b)). Wind speed recorded at Cape Enragé is also shown (courtesy Atmospheric Environment Service, Bedford).

Month	Cape Maringouin		Cape Enragé		
	Height(m)	Period(s)	Height(m)	Period(s)	Wind Speed (km/h)
May, 1978	—	—	—	—	23.5
June	0.33	4.94	0.35	4.99	17.3
July	0.33	5.05	0.26	4.54	13.3
August	0.32	5.64	0.33	4.31	17.8
September	0.42	4.42	0.56	4.47	19.2
October	0.41	4.63	0.62	4.56	18.7
November	0.38	4.32	0.65	4.81	28.8
December	0.40	3.94	0.85	5.79	—
January, 1979	—	—	0.82	5.54	—
February	—	—	0.73	4.65	—

waves over a fetch of approximately 140 km. Waves propagate from the Bay of Fundy into Chignecto Bay. They are greatest in Chignecto Bay but are nevertheless significant at the heads of Shepody Bay and Cumberland Basin because of the alignment of the system with the dominant southwesterly winds. Table 4 synthesizes the wave measurements made in this study based on data presented by Marine Environmental Data Services (1979a, b). These data are shown graphically in Figure 17. Wave conditions are most severe at the mouth of the system and decrease landward. The peak significant wave height and period for the outer and inner stations are 3 m and 10 seconds and 2 m and 8 seconds, respectively. Waves 2 m in height have been observed at the heads of both Shepody Bay and Cumberland Basin breaking over mud flats and resulting in the production of salt marsh cliffs (Desplanque,

pers. comm., 1989). Wave conditions are highly variable with time (Fig. 18). Most severe conditions occur during the passage of winter cyclones (Lewis and Moran, 1984) that occur principally during the months of November and January and last up to 2 days. In Figure 18, the measured significant wave height for the month of November, 1979 is illustrated together with the critical heights for sediment resuspension in the outer and inner bay. There were 9 resuspension events during that month in the outer bay and 10 in the inner bay. These events resulted in the release of fine grained sediments from the seabed.

#### TEMPERATURE AND SALINITY

Water temperature in Chignecto Bay varies by approximately 18°C throughout the year (Fig. 19). The greatest var-

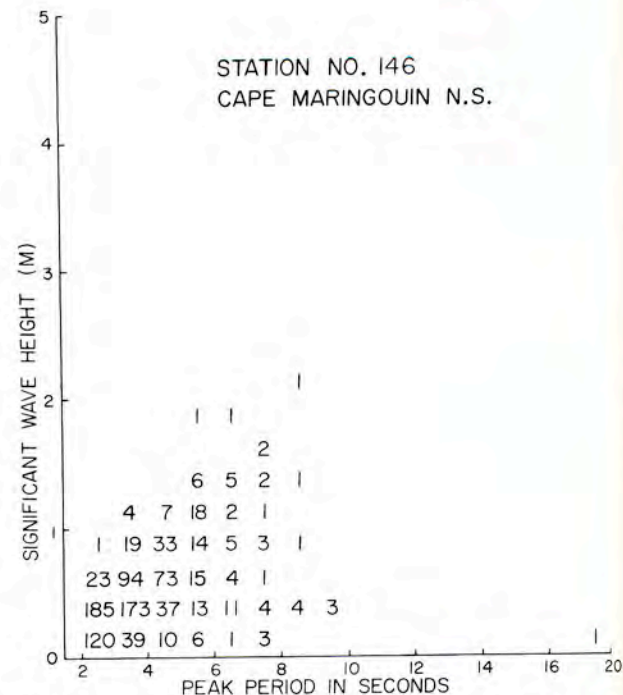
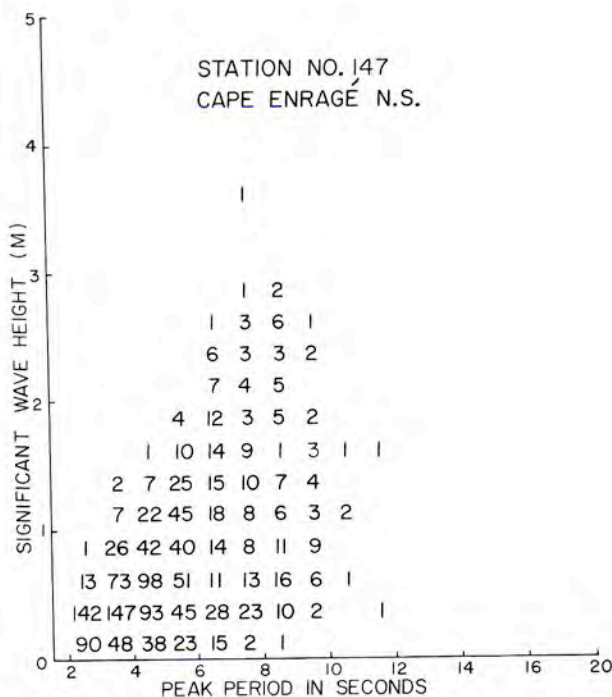


**Figure 17.** A scattergram of significant wave height and peak periods measured at the two waverider buoy sites (Fig. 2) during 1978. Note the significant attenuation in wave height from Cape Enragé to Cape Maringouin with no change in period.

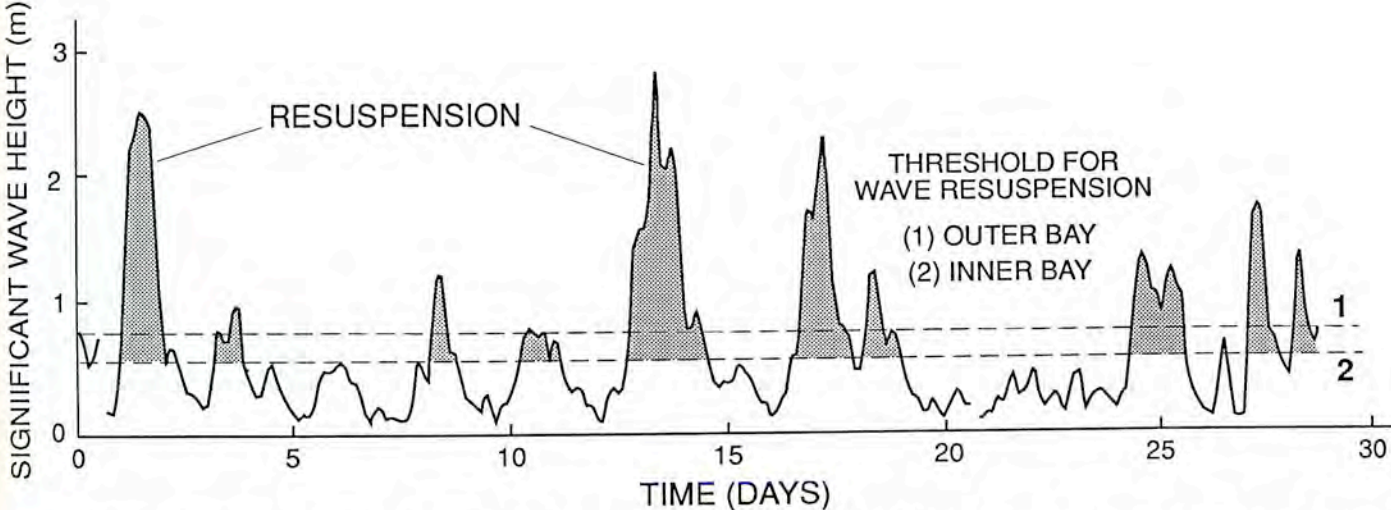


**Figure 18.** A time-series plot of the significant wave height for November, 1978 recorded at Cape Enragé with the observed threshold for sediment suspension superimposed. Note the irregular influences of waves and the approximate 1-day duration of most storms. This may explain the lack of cyclicity in the tidal rhythmites of sediments illustrated in Figure 8.

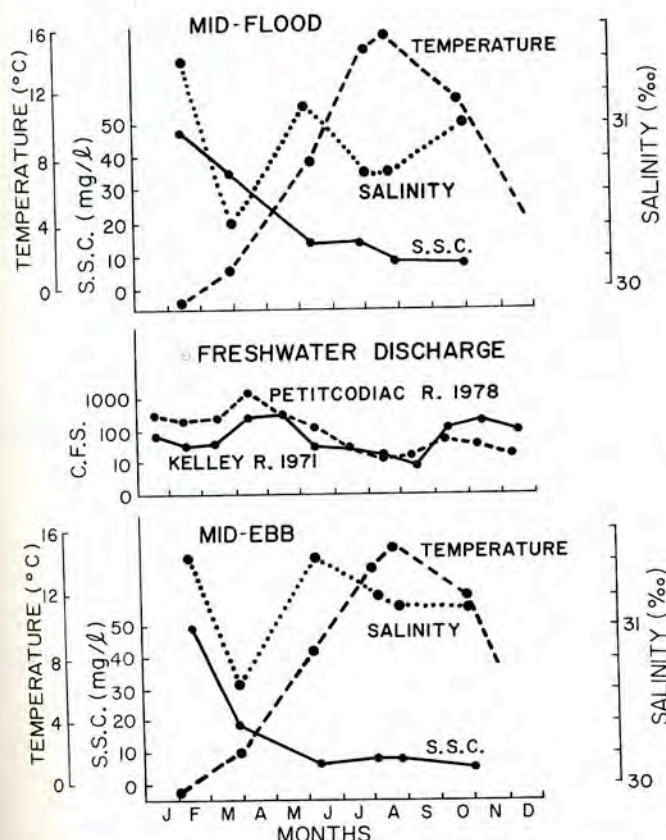


**Figure 19.** A synthesis of seasonal mean values of water temperature, salinity and suspended sediment concentration during mid-flood and mid-ebb conditions in Chignecto Bay. Seasonal inputs of fresh water from the two largest rivers entering Chignecto Bay (the Petitcodiac and Kelley rivers; see Fig. 1 for location) are also shown. Note that the highest values in SSC occur during late winter/early spring and decrease steadily throughout the year. Lowest salinities correspond to maximum river discharges.

iation occurs at the head of the system where temperature drops to  $-1.5^{\circ}\text{C}$  during January/February and reaches  $17^{\circ}\text{C}$  during mid-August. This is because of heat transfer between the water column and expansive littoral zone. In outer Chignecto Bay, the temperature varies from  $-1.3^{\circ}\text{C}$  to  $14.5^{\circ}\text{C}$ . Here, the variation over a tidal cycle is approximately  $1^{\circ}\text{C}$ ; farther landward the variation is up to  $2^{\circ}\text{C}$ . During winter, there is a temperature gradient dipping landward that produces the highest water temperatures around the time of high water. During the summer, the converse is true; temperature decreases seaward and highest temperatures occur around low water due to solar heating of the tidal flats (Fig. 15A).

The vertical variation in temperature is small as a result of strong tidal mixing (Garrett *et al.*, 1978). In the inner bay, waters are well mixed except during stillstands of the tide, when surface solar heating can take place. In the outer bay, there is a systematic decrease in temperature from the surface to the seabed of approximately  $1^{\circ}\text{C}$ . This gradient is apparent throughout the entire tidal cycle.

Sea water density variations in Chignecto Bay are controlled largely by variations in salinity. Consequently, the effects of fresh water runoff have a strong impact on stratification, ice formation and ice melting (Gordon and Desplanque, 1983). The source of fresh water is in the inner bay. Consequently, the salinity gradient shows a steady increase down the estuary. This increase persists throughout the year. The lowest salinities occur during low water. Typical midsummer salinities are 31 ppt at the mouth of Chignecto Bay and 29 to 30 ppt at the mouths of Shepody Bay and Cumberland Basin (Fig. 15b; Holloway, 1981). Typical springtime salinities are 26 to 30 ppt. Salinity gradients are higher in the upper bay than in the lower bay. Salinity fluctuations over a tidal cycle during midsummer are 0.6 to 0.4

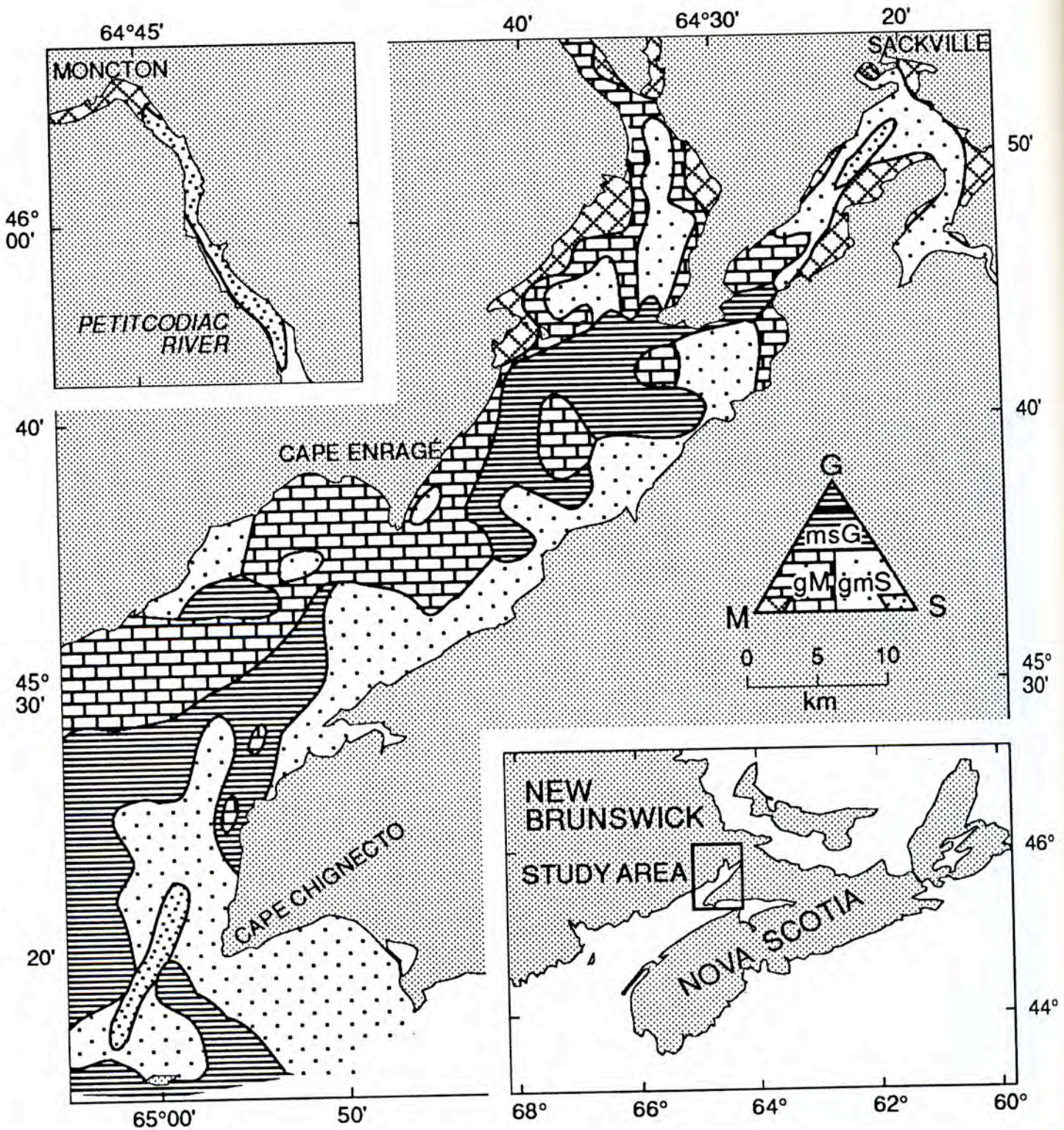


**Figure 20.** A textural classification of the bottom sediments in Chignecto Bay (M, mud; S, sand; G, gravel). The correspondence between this map and the surficial geological map (Fig. 13) is poor. This may be due to the dominating influences of ice-rafting of gravel over the hydrodynamic sorting processes.

ppt. A weak salinity stratification occurs throughout the system during the summer; surface salinity being 0.3 ppt less than that of bottom waters. At the mouth of Chignecto Bay, stratification is less near the coast than near its centre (Tee, 1982).

A large volume of fresh water flows into Chignecto Bay during early spring, significantly reducing salinity (Fig. 19). A curious mid-depth minima (by 2 ppt) also results (Fig. 22 in Amos and Asprey, 1981). This causes an instability of the water column of the inner bay (density variation approximately  $1.5 \times 10^{-9} \text{ g/m}^3$ ). The density variation due to changes in suspended sediment concentration with depth is small ( $2 \times 10^{-10} \text{ g/m}^3$ ). The water column of the outer bay is stable at all times, with salinity increasing with depth.

PRESENT SEDIMENTARY CHARACTER

THE DISTRIBUTION OF SEDIMENTS

*Bottom Sediments*

The distribution of bottom sediment in the Chignecto Bay system is shown in Figure 20. A complex distribution of varying sediment types is evident, which bears a weak relationship to the underlying surficial geology shown in Figure 13. Gravel and muddy, sandy gravel dominate the outer and axial parts of Chignecto Bay. Gravelly, muddy sands prevail along the eastern margin of Chignecto Bay and the axial parts of Shepody Bay and Cumberland Basin. Gravelly muds and sandy muds are found along the western margin of Chignecto Bay, throughout Shepody Bay and in isolated patches elsewhere. Muds predominate on the littoral margins of Shepody Bay and Cumberland Basin and are least abundant in the sublittoral regions. Clean sand occurs only in the Petitcodiac River region of Shepody Bay, along the eastern margin of Chignecto Bay and off Cape Chignecto. In general, the bottom sediments are poorly sorted and multimodal, and commonly contain a gravel-sized component. Figure 21A, B shows the percentages of sand and gravel, respectively, in bottom sediments of the Chignecto Bay system. Note the lateral asymmetry in sediment distribution: sand predominates in the eastern margin of the system and conversely, fines predominate in the western margin. Gravel is ubiquitous, though it maximizes along the central axis of the bay and at the mouth.

Heavy minerals in the sand-sized range constitute between 2 and 3 per cent by weight of bottom sediments and are made up of volcanic rock fragments and ferromagnesian minerals (principally pyroxenes, amphiboles and garnet; Hussain, 1980). No clear spatial segregation of heavy minerals is apparent within Chignecto Bay, and therefore the role of hydrodynamic processes in sorting sand-sized bed sediment is considered minor. Hussain (1980) has correlated many of the attributes of the heavy minerals to those in the rocks surrounding the bay. He showed that the heavy minerals were generally close to source. The abundance of the metastable minerals is diagnostic of an adjacent cliff source

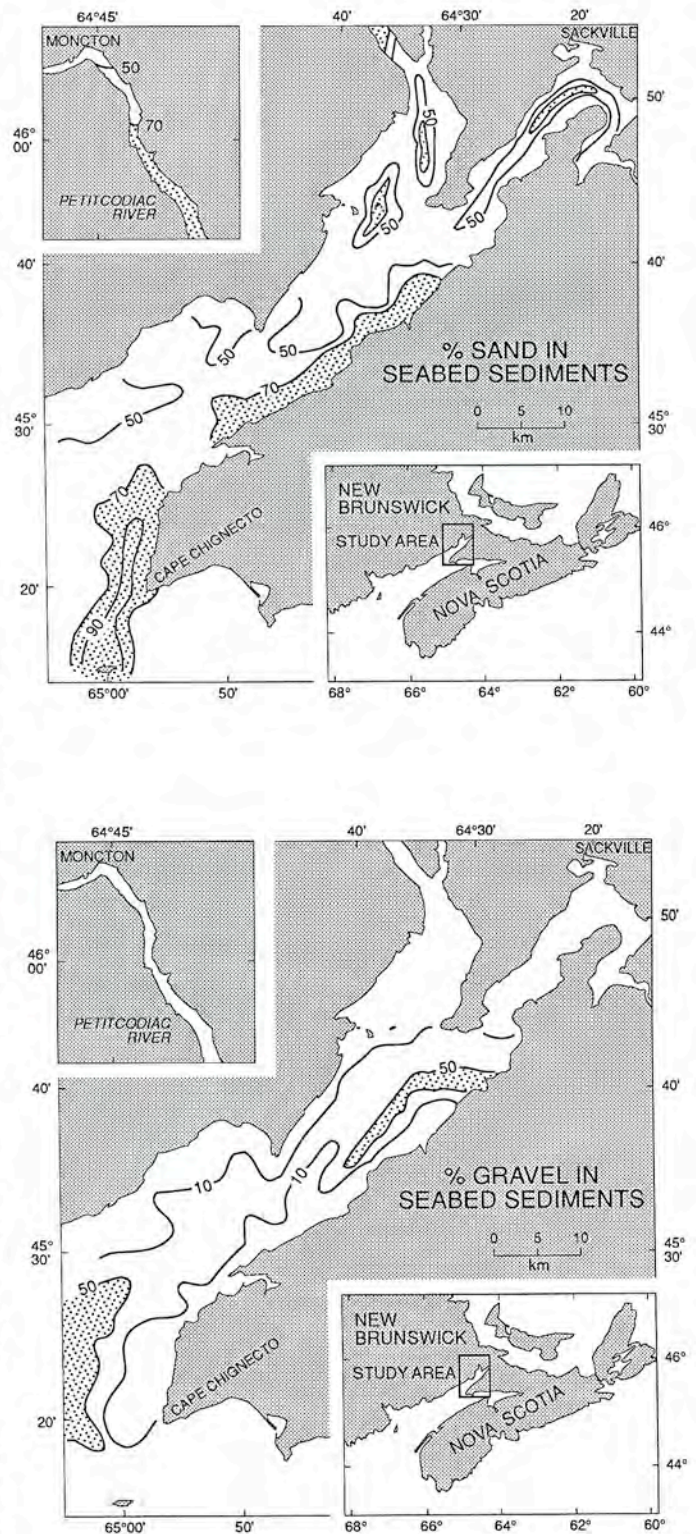
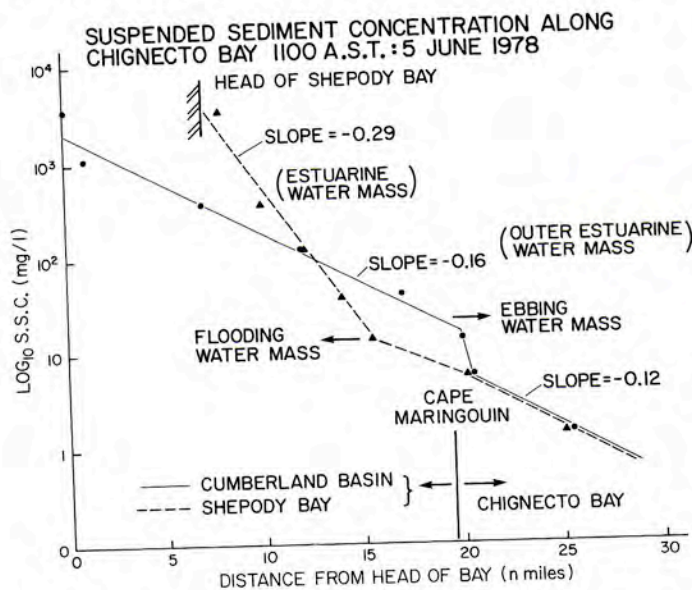


Figure 21. The percentages of sand, and gravel measured in seabed samples taken from Chignecto Bay. Sand predominates in the eastern portion of the bay and is derived from coastal erosion of glaciodeltaic deposits. Gravel is abundant along the median of the bay, where it forms a lag deposit derived by hydraulic winnowing of ice-rafted debris.

with little subsequent reworking. At the mouth of Chignecto Bay, heavy minerals comprise up to 10 per cent of the bottom sediments and are associated with well-sorted, wave-reworked sand or gravel. This illustrates that here, hydrodynamic sediment sorting and winnowing has taken place.

### Suspended Sediments

The suspended sediments of Chignecto Bay form a complex pattern of turbid fronts, ribbons, plumes and boils diagnostic of resuspension, dispersion and advection. Under fair-weather conditions, the suspended sediment concentration (SSC) shows an exponential decrease seaward from a predicted maximum of around 68 g/L (Amos and Tee, 1989). The gradient in concentration has been observed by Keizer *et al.* (1984) and Dewolfe *et al.* (1990) in Cumberland Basin, by Topliss *et al.* (1990) in Shepody Bay and by Amos and Topliss (1985) in Chignecto Bay. It is also present in Minas Basin, and the Avon River Estuary (Amos and Tee, 1989). The exponential gradient persists in time, though the slope varies in a direct relationship with the concentration at the turbidity maximum and wave activity, which are both seasonal. The gradient appears to be a balance between sediment input at the head of the estuary (through river input and wave erosion) and the combined effects of dispersion seaward by longitudinal tidal mixing and deposition along the estuary (Amos and Tee, 1989). An example of the concentration gradient is shown in Figure 22. Here, the intrusion of the Cumberland Basin turbid plume into Chignecto Bay during the ebb tide is expressed by an offset in the sediment gradient at a turbid front (Amos, 1987). A similar turbid front occurs between the flooding water masses of



**Figure 22.** The width-averaged surface suspended sediment concentration measured along the axes of Shepody Bay, Cumberland Basin and Chignecto Bay at 1100 AST on 5 June, 1978. The exponential decrease in SSC is clear in the figure, together with the sharp inflection points at the boundary of water masses.

Shepody Bay and Chignecto Bay and results in an inflection point in the concentration gradient.

There is a large seasonal variation in SSC in all three bays. It is highest during ice breakup, which usually occurs in February or March, and least during the winter months of December and January (Fig. 19). SSC decreases steadily throughout the summer as a result of deposition on the littoral mud flats (Hildebrand *et al.*, 1980), but increases again during the autumn (October and November) as a result of wave resuspension. Observations made by Hildebrand *et al.*, (1980) in Cumberland Basin show a six-fold increase in SSC (from 500 to 3,000 mg/l) associated with an increase in wave height from 0.15 to 0.5 m. Waves may thus be very important to mud flat stability even in the inner parts of high-energy, macrotidal estuaries.

The spatial distribution of surface suspended sediments, discriminated using the Landsat MultiSpectral Scanner (Munday *et al.*, 1980), is illustrated in Figure 23. The figure shows examples of turbid fronts, turbid ribbons and turbid plumes. Turbid fronts and turbid ribbons are diagnostic of the boundaries of water masses commonly separated by shear planes. These planes were often detected during anchor stations. When they crossed the ship's location, significant and abrupt changes in the character of the water column occurred.

The vertical distribution in SSC varies considerably. In outer Chignecto Bay, stratification in SSC occurs throughout the entire tidal cycle and shows a decrease in concentration in proportion with the logarithm of height above the bed. Elsewhere in the system, stratification in SSC occurs immediately after the stillstand of tidal flow (high and low water), but the water column is mixed during peak flows (Fig. 15D). This settling can result in a 2 to 8 times enrichment in bottom water SSC over surface waters. The observed ratio of surface-to-depth-averaged suspended sediment concentration, averaged over all observations, was  $0.57 \pm 0.26$  (Amos and Tee, 1989). This result is substantiated by work carried out throughout Cumberland Basin by Dewolfe *et al.* (1990).

Increases in SSC due to wave resuspension have been observed throughout the system. Wave heights in excess of 0.5 m resuspended material in the inner part of Chignecto Bay, whereas waves in excess of 0.7 m in height resuspended material in the outer estuary (Amos and Asprey, 1981). Still water settling experiments made on this material in a bottom-withdrawal tube showed that the concentration half-life was  $6.4 \pm 1.2$  minutes and that particles coarser than 20 microns were first to deplete forming tidal couplets in regions of high turbidity ( $> 200$  mg/l).

Electron microscopic examination (using a Cambridge Stereoscan 180) of the material suspended in Shepody Bay and Cumberland Basin indicated that less than 5 per cent of particles are flocculated, and between 85 and 95 per cent are inorganic. The majority (70-90%) of this material comprises fine-silt-sized, angular, lithic fragments. Coulter Counter analysis of the size spectra showed the model size of

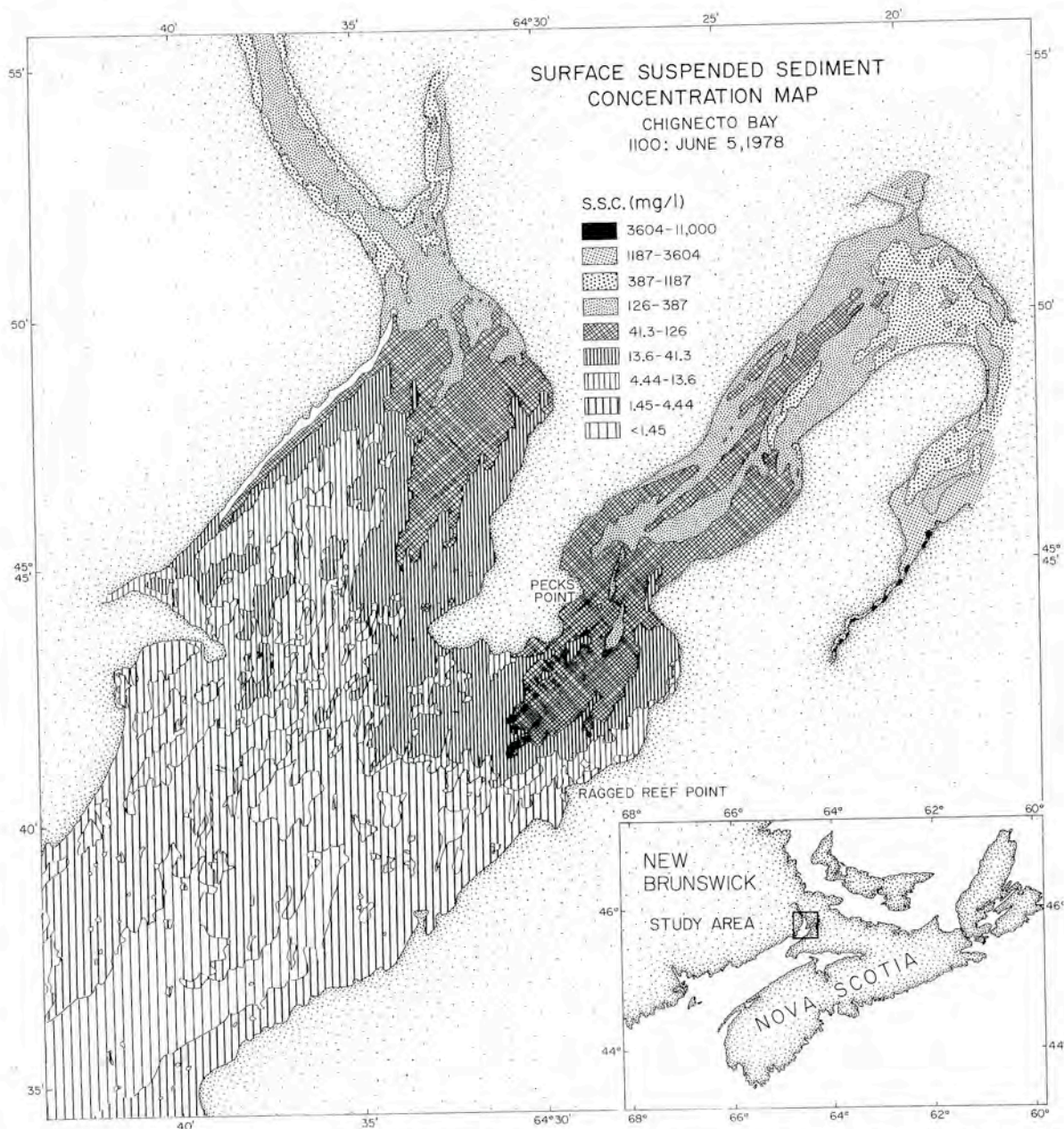


**Figure 23.** A thematic plot of surface suspended sediment concentration in the upper part of the Chignecto Bay system. The image was created from Landsat Multi-Spectral Scanner data recorded at 1100 AST on 5 June, 1978. The image coincides with the measurements shown in Figure 22. The isopleths of SSC show a seaward deflection in the zones of ebb dominance and a landward deflection in zones of flood dominance. The irregular pattern of isopleths in Shepody Bay may result from localized resuspension of bed sediment.

suspended sediment to range from 10 to 30 microns over all stages of the tide (Figure 24). The clay content of suspended material, unlike other estuaries, is constant at 20 per cent along the length of Shepody Bay. Chignecto Bay, however, demonstrates a gradient in silt content of suspended material that decreases inward from a peak of 80 per cent at the mouth. Isolated measurements of suspended clay content made during October to November, 1978 in the inner, western part of the Chignecto Bay were up to 80 per cent. This anomaly is considered to be the result of wave resuspension

(see Fig. 18) of early Holocene muds (G2) that here constitute the seabed. Analysis of particle character was made on near-surface and near-bed samples taken over a tidal cycle at station 19 (mouth of Cumberland Basin during calm conditions). There were no obvious correlations between grain size and stage of the tide (Fig. 25). However, an enrichment in silt content by 20 per cent was evident in the bottom waters. Note that no sand was suspended during the peak tidal flows (0.5 m/s) despite its presence at the bed.

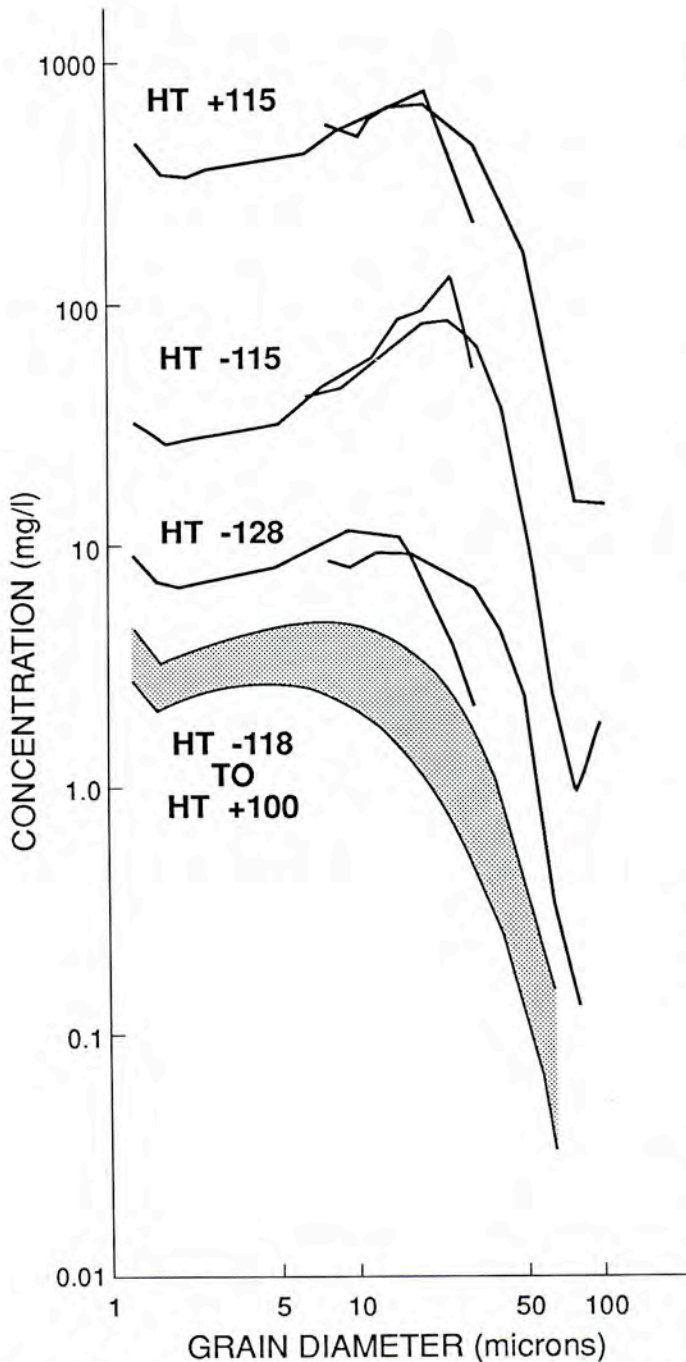


**Figure 24.** The grain size spectra of suspended sediments sampled over tidal flats near the mouth of Cumberland Basin on 7 November, 1979 at various times (in minutes) before and after two local high tides (HT). Note that the modes in the spectra occur at between 10 and 30 microns and a nearly even distribution in sizes finer than the mode. Almost no sand was detected in suspension.

#### SOURCES OF SEDIMENT

##### Cliff Erosion

Wave erosion of the cliffs bordering Chignecto Bay provides an abundant source of sediments to the system. The mean recession rates of the cliffs bordering Shepody Bay, Cumberland Basin and Chignecto Bay, evaluated between

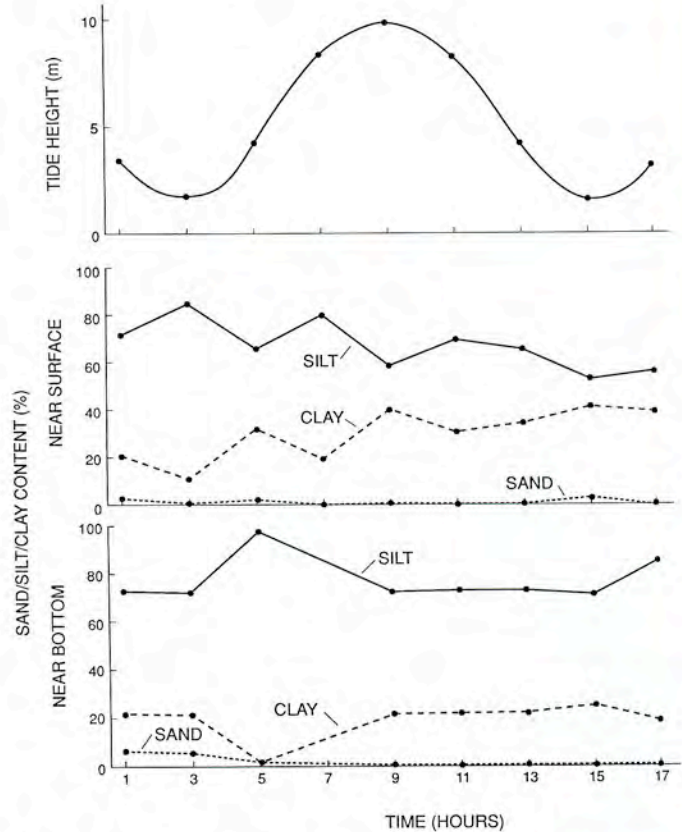


**Figure 25.** The percentages of suspended sand, silt and clay measured from scanning electron micrographs of surface and near-bed samples each taken two hours over a tidal cycle at the mouth of Cumberland Basin (Fig. 2, Station 19). Note the increase in silt content with depth, the lack of any obvious correlation between sediment texture and tidal stage, and the virtual absence of sand. No waves were present when these measurements were taken.

1947 and 1975, were 0.19, 0.20, and 0.37 m/a, respectively. The highest erosion rate (1.0 m/a) occurs in regions of greatest wave exposure, such as the western side of Chignecto Bay and the mouths of Cumberland Basin and Shepody Bay. The total volume of sediment released by coastal erosion is estimated to be  $1.03 \times 10^6$  m<sup>3</sup>/a (Fig. 26). The majority of this material is derived from the volcanic rocks of outer Chignecto Bay (20 m<sup>3</sup>/m/a) where cliff heights (50 m) and wave exposure are greatest. The highest rate of cliff erosion occurs during periods of highest waves. This is typically during the months of December and January. Sediment so derived is predominantly in the silt size range (Chalmers, 1894).

##### Rivers

The total quantity of inorganic sediment entering the system from fluvial sources was determined from information gathered at the hydrometric stations illustrated in Figure 1. The figure also shows the catchment area of the system: 5014 km<sup>2</sup>. The total input of fresh water is  $3.14 \times 10^5$  m<sup>3</sup>/a (Hildebrand *et al.*, 1980) and the maximum discharge of the largest river (the Petitcodiac River) is 37 m<sup>3</sup>/s (Fig. 19).



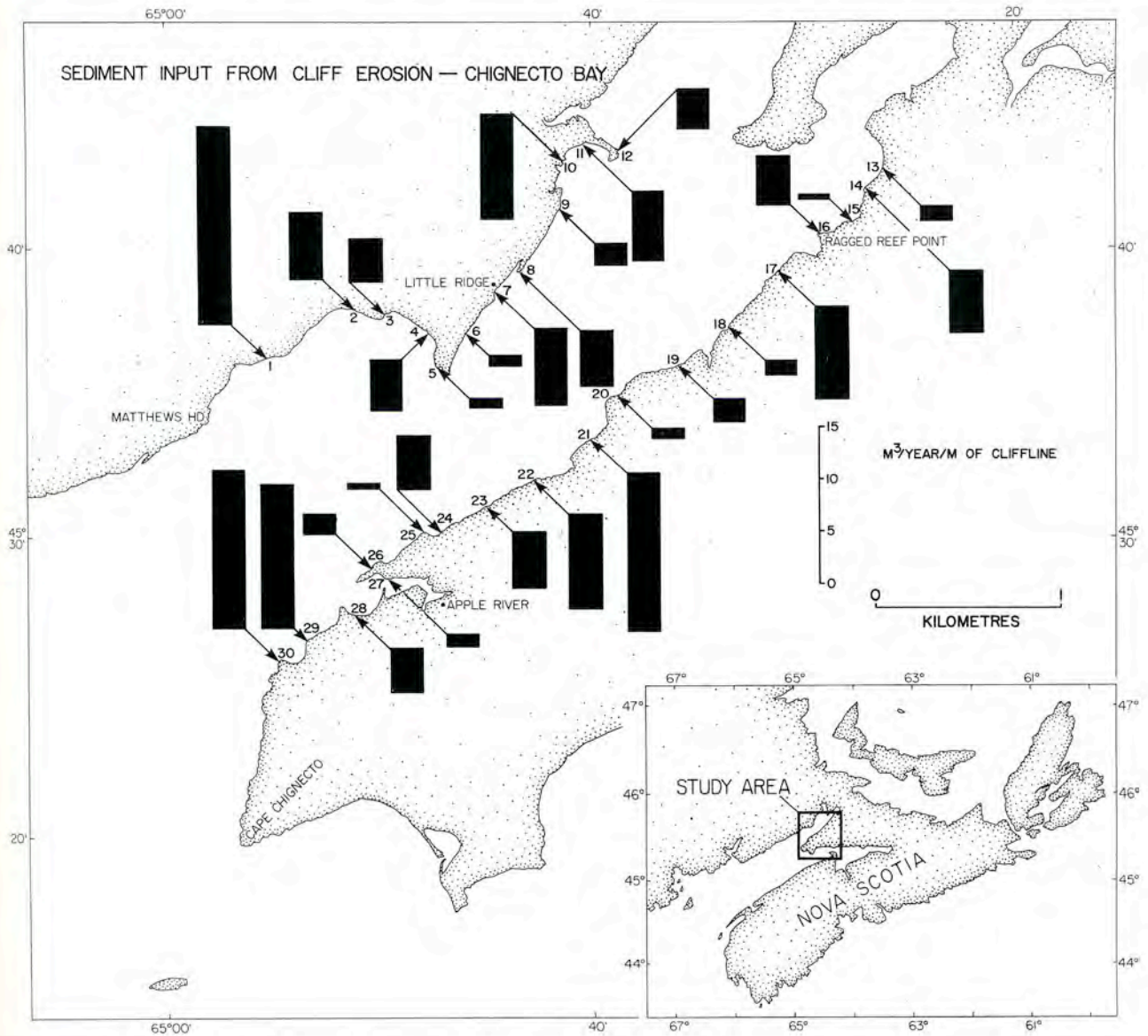


Figure 26. The sediment input to Chignecto Bay through cliffline erosion. Note that the majority of sediment is derived from the outer part of the bay where cliffs are highest and wave forces greatest.

Sediment concentrations in river water are typically less than 2 mg/l and rarely exceed 10 mg/l. The mean fluvial sediment input to the Chignecto Bay system is  $3.5 \times 10^5$  m<sup>3</sup>/a or 67 m<sup>3</sup>/km<sup>2</sup>. The majority of this is introduced to the system in suspension during spring floods in the months of March and April. Total fluvial input of sediment is 30 per cent of that derived from cliff erosion. The fluvial material is in the silt-clay size range.

*The Bay of Fundy*

An estimate of the exchange of sediment with the Bay of Fundy has been attempted by the establishment of 3 anchor stations at the mouth of Chignecto Bay (stations 12, 13, 14, Fig. 2). Residual fluxes of suspended sediment derived from these stations indicate a net export of sediment

of  $5.5 \times 10^6$  m<sup>3</sup>/a during fair-weather conditions. According to Amos (1987) a further volume of  $1.8 \times 10^6$  m<sup>3</sup>/a is discharged during storms. A large part of this material is derived from seabed erosion off Cape Enragé. The bathymetry in this region shows a deepening by 20 m between the original Admiralty survey conducted in 1861 and the latest survey carried out during this project in 1979 (courtesy Canadian Hydrographic Service). Here, approximately  $6.0 \times 10^6$  m<sup>3</sup> of fine material is released to the water column annually. A net export of sediment to the Bay of Fundy is verified qualitatively in Landsat and NIMBUS-7 images, which show turbid plumes extending from Chignecto Bay along the northwestern shore of the Bay of Fundy and over a region mapped by Fader *et al.* (1977), Swift *et al.* (1973) and Loring (1982) to be underlain by fine grained sediment.

## TRANSPORT OF SEDIMENT

*Bedload Transport and Deposition*

The bedload transport of sediment was inferred from bedform type and orientation based on sidescan imagery of the seabed. A synthesis of the interpretation of this imagery is shown in Figure 27. Along the western margin of Chignecto Bay between Cape Enragé and Cape Maringouin, there is a suite of flood-oriented sand waves and 2-dimensional and 3-dimensional megaripples. This suite occurs in a region of peak tidal flow that varies between 1.0 to 1.5 m/s (Fig. 14). The central regions of the estuary are void of large-scale bedforms as a result of the paucity of sand. Flood-oriented comet marks are, however, abundant. This region is subject to peak tidal flows between 1.5 and 2 m/s. There is a trend of increasing bedload transport from the western margin of the bay (rippled plane bed) to its centre (sand waves and

2-dimensional megaripples) that parallels the increase in peak flow to 1.5 m/s. Above this flow, sand is presumed to be removed by intermittent suspension.

A band of irregularly spaced sand ribbons occurs parallel to the eastern margin of Chignecto Bay. Superimposed on the sand ribbons are poorly-developed, flood-oriented, 2-dimensional megaripples. The absence of well-defined slip faces and the high fines content of the constituent sediment suggests that the Chignecto Bay bedforms are at the feather-edge of unit R and are consequently sediment starved (the fines derived from the underlying unit). Large-scale bedforms in Shepody Bay and Cumberland Basin are restricted to the median line of the outer parts. Here, flood-oriented, 2-dimensional and 3-dimensional megaripples and comet marks attest to a headward transport of sand in regions where the peak flow is below 1.5 m/s. Above 1.5 m/s, sand flats occur as upper flow plane beds with flow-parallel lineations.

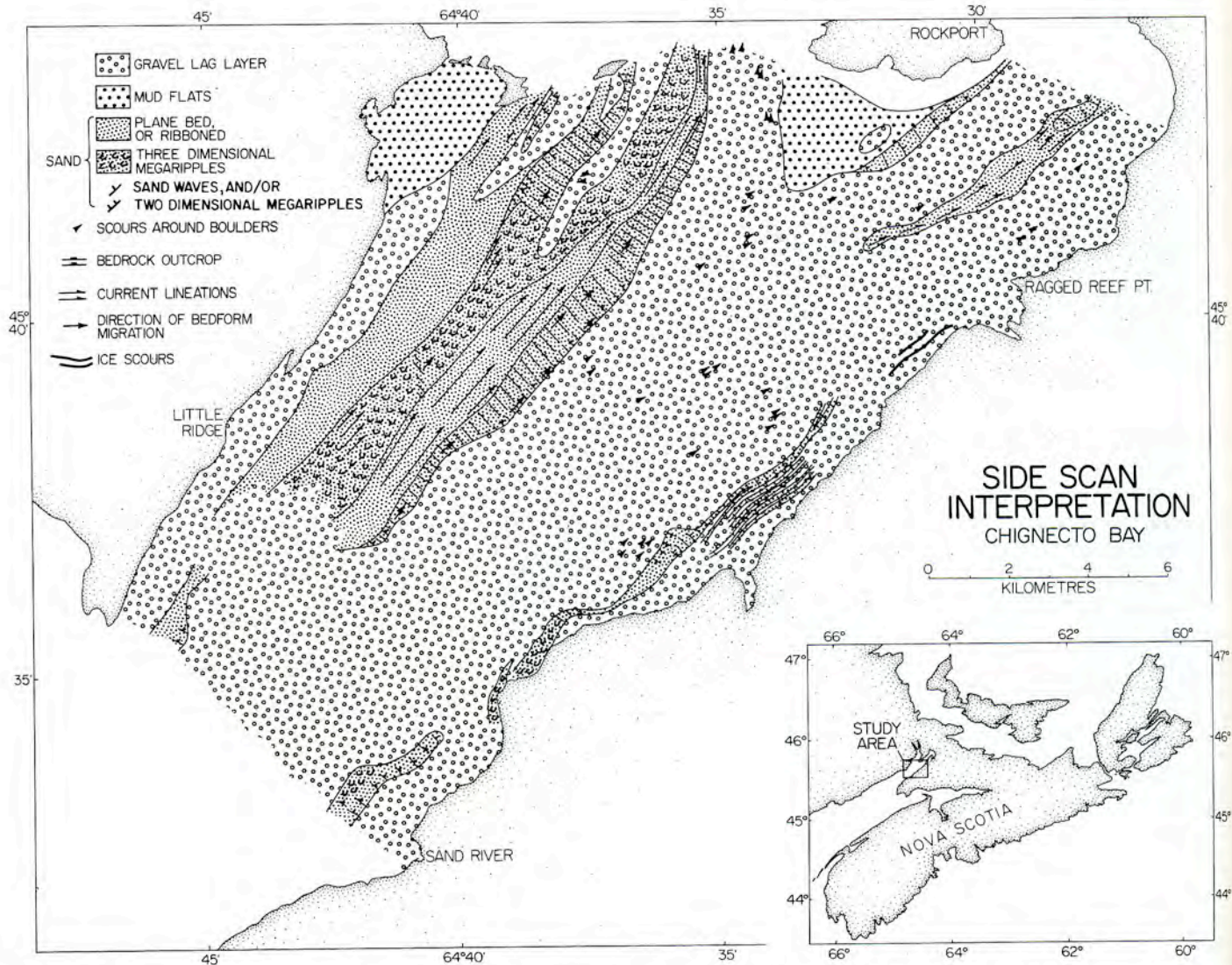


**Figure 27.** The interpretation of surficial bed features detected on sidescan sonograms of Chignecto Bay. The suite of flood-oriented bedforms along the western margin of the bay is evident. The remainder of the bay is devoid of bedforms with the exception of isolated sand ribbons along its eastern margin and at the mouth of Cumberland Basin.

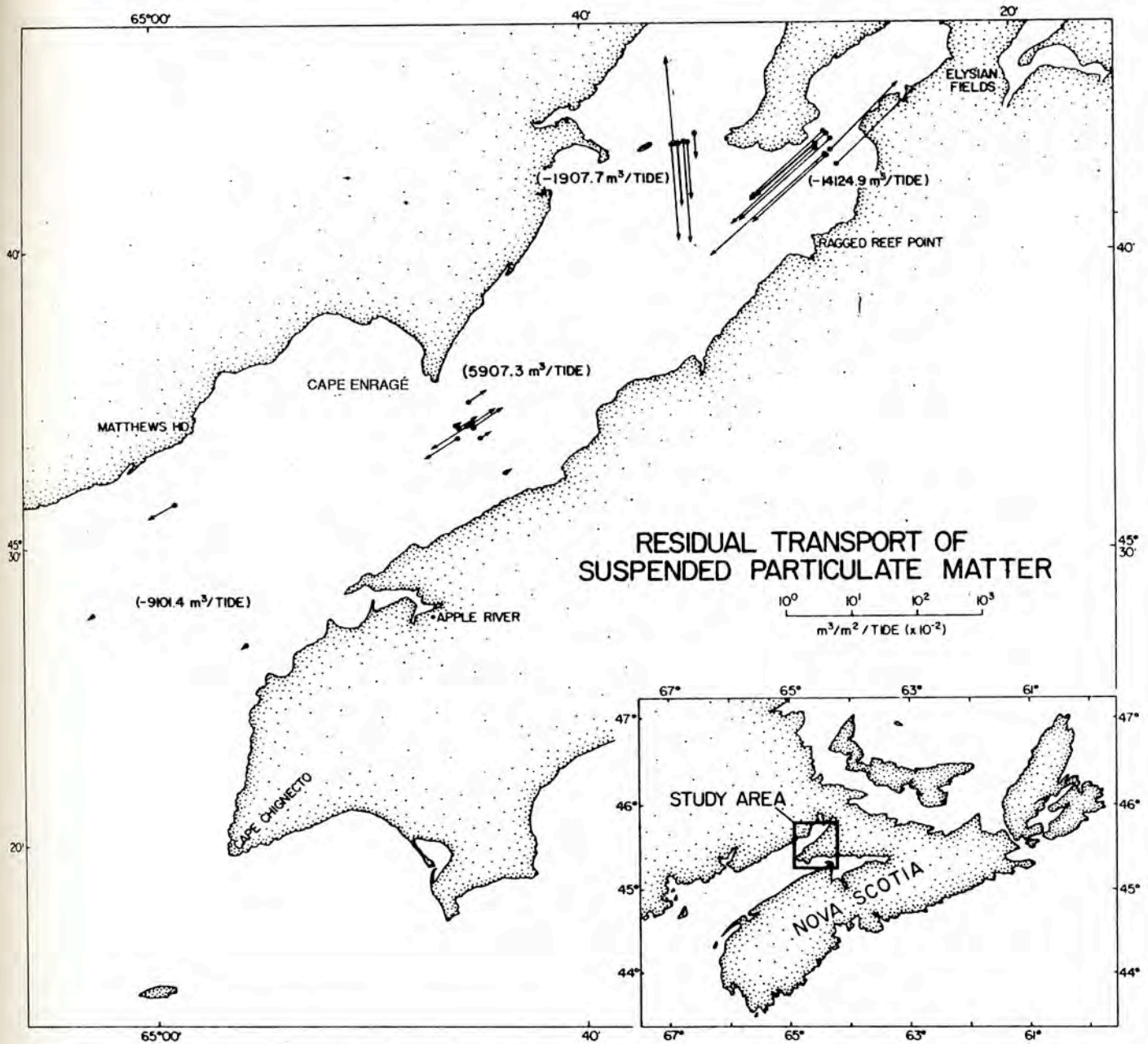


**Figure 28.** The residual transport of suspended particulate matter in the Chignecto Bay system measured over single tidal inundations at seven periods of the year (see Amos and Asprey, 1981 for details). Each value is the product of measured SSC and velocity integrated with depth and time for the duration of observations (normally 15 hours). The values in brackets denote first estimates of the mass balance of sediment across the sections on which they are found. Positive values denote import, negative values denote export. Note the strong export of sediment throughout the system except near Cape Enragé. Here, results are confused by the effects of wave resuspension. Almost 50 per cent of stations showed some wave effects on SSC.

#### *Suspended Sediment Transport and Deposition*

The flux of suspended sediment has been estimated for Chignecto Bay by Amos and Asprey (1981) for the stations illustrated in Figure 2. A brief review of these data is given by Amos (1987). A synthesis of the results is shown in Figure 28. Sediment budget assessments of Chignecto Bay indicate that a total of  $7.3 \times 10^6$  m<sup>3</sup> of sediment is released annually, of which  $1.3 \times 10^6$  m<sup>3</sup> is derived from external sources (rivers and eroding cliffs) and the remainder is derived from

bed erosion. Based on the volume of the Recent deposits in Chignecto Bay, it is calculated that sand and gravel are being introduced into Chignecto Bay at a rate of  $8 \times 10^4$  m<sup>3</sup>/year. This is approximately 7 per cent of the annual influx of sediment to the system and only 1 per cent of the total volume of material in transport. Thus the major part of material in transport is in the silt or clay size range and has been demonstrated to be transported in suspension or intermittent suspension.

The trapping efficiency of the Chignecto Bay system (defined after Schubel and Carter, 1984) is very low as a result of the reclamation of fringing salt marshes (Amos and Tee, 1989) and high wave activity. That which is released into the system (by seabed erosion, fluvial discharge and cliff erosion) can be assumed to be ultimately exported to the Bay of Fundy.

In the inner estuary, the pattern of suspended sediment transport is unclear. Measurements at the mouths of Shepody Bay and Cumberland Basin show both import and export through time. This pattern is in response to changes in SSC and SSC gradients. Amos and Tee (1989) showed that the total suspended mass in Cumberland Basin remained remarkably constant throughout two years of observations ( $10^{11}$  g or approximately  $3.8 \times 10^4$  m<sup>3</sup>) despite changes in SSC patterns due to fluvial input, ice and wave reworking and mud flat sedimentation (Keizer *et al.*, 1984). We propose that exchanges at the mouth of Cumberland Basin occur that maintain the total mass in suspension and the equilibrium gradient constant and in proportion with the energetics of the system.

#### SUMMARY AND CONCLUSIONS

The Chignecto Bay system, Bay of Fundy, is dominated by fine grained sediments and suspended sediment transport because of the fine grained nature of the Paleozoic rocks on which the system sits and because of the present-day erosion of the fine grained, unconsolidated sediments that underlie much of the bay. It clearly differs from the Minas Basin, which is dominated by sand-sized sediment and bed-load transport due to the erosion of Triassic sandstone cliffs surrounding that Basin (Amos and Long, 1980).

The unconsolidated sequence in Chignecto Bay is composed of up to 50 m of glacial and postglacial deposits that are predominantly fine grained in texture. These formed largely in a sublittoral setting under conditions of sea level, tidal range and wave exposure dramatically different from those of today. Two periods of microtidal conditions are recognized separating two periods of macrotidal conditions interpreted to have occurred during the last 13,300 years. A period of regression took place from 13,300 to 7000 BP. A brief period of macrotidal conditions 12,000 BP was responsible for the development of a sand and gravel unit (G3) that underlies much of the bay and is thickest between Matthews Head and Apple River (Fig. 4).

A lowstand of relative sea level is recognized to have occurred circa 7000 BP at 25 m below present sea level. At this time, an extensive low-gradient, mud-dominated littoral flat (G2) is interpreted to have developed north of Cape Enragé. This flat is dominated by point bar lateral accretion bedding associated with littoral creek migration (Smith, 1989). A lack of wave-formed structures in this unit suggests that the estuary was sheltered from the outer Bay of Fundy by a barrier at the estuary mouth. The deposition of fines would have taken place in the back-barrier lagoon situated in the central and inner paleoestuary. Here inclined heterolithic

stratification predominated. A clay-rich salt marsh fringed the mud flats at the approximate positions of the mouths of Cumberland Basin and Shepody Bay. The facies of unit G2 bear only weak similarities to the tidal flats of the North Sea reported by Terwindt (1981) and Nio and Yang (1989). For example, we found no evidence of cyclicity in lamina thickness diagnostic of tidal bundles. Also, we found no evidence of large-scale crosslamination diagnostic of large-scale bedforms and the associated reactivation surfaces. This was likely due to the paucity of sand in the central estuary at the time. We presume the sand (if available) was deposited in the mouth of the paleoestuary (close to that of today) in the form of bars and ebb tidal deltas such as those reported from outer Cobequid Bay (Dalrymple, pers. comm., 1990).

A steady increase in tidal range prevailed throughout the late Holocene transgression of Chignecto Bay. Unit G1 was deposited during early stages of this transgression. The dominance of lenticular and flaser bedding is diagnostic of the increasing influence of tidal currents between 6,000 and 3,000 BP.

At 3,000 BP there was a significant change in depositional environment, possibly associated with overtopping of the outer estuary barrier and associated deposits. The depocentre shifted from the central estuary to the inner estuary, with littoral deposition of fringing mud flats and salt marshes. The central estuary became a region of erosion of units G1 and G2, and slow development of a sand and gravel facies (R).

The distribution of facies in the unconsolidated sequence in Chignecto Bay is summarized in Figure 29. Note the lateral asymmetry in facies distribution. The laminated facies associated with G2 point bar accretion deposits predominates in the eastern estuary and is virtually absent in the west. Lenticular and flaser bedding, generally associated with medium-energy, mesotidal deposits of unit G1 and diagnostic of tidal activity, prevail in the western part of the estuary and are virtually absent from the extreme east. The sand and gravel associated with modern-day processes does not correlate well with the acoustic unit R. The absence of this unit in eastern Chignecto Bay is a result of a lack of contrast with the underlying units likely due to the absence of large-scale bedforms. There is a reversal of the depocentre from that of unit G1 to the eastern part of the estuary. The reason for the asymmetry is unclear, but may be related to estuarine paleobathymetry and the resulting complex patterns of tidal flow.

Modern, sandy sediments account for only 1 per cent of the total budget of sediment. Net input of Recent sediment is  $1.3 \times 10^6$  m<sup>3</sup>/a. Approximately 93 per cent of this volume is composed of fine grained sediment; the remainder is sand and gravel. The majority comes from cliffline erosion ( $1.03 \times 10^6$  m<sup>3</sup>/a) while rivers supply  $3.5 \times 10^5$  m<sup>3</sup>/a. The fine grained sediment is quickly transported through the system in suspension by strong residual currents (Tee and Amos). Results of accretion/erosion on the mud flats at the

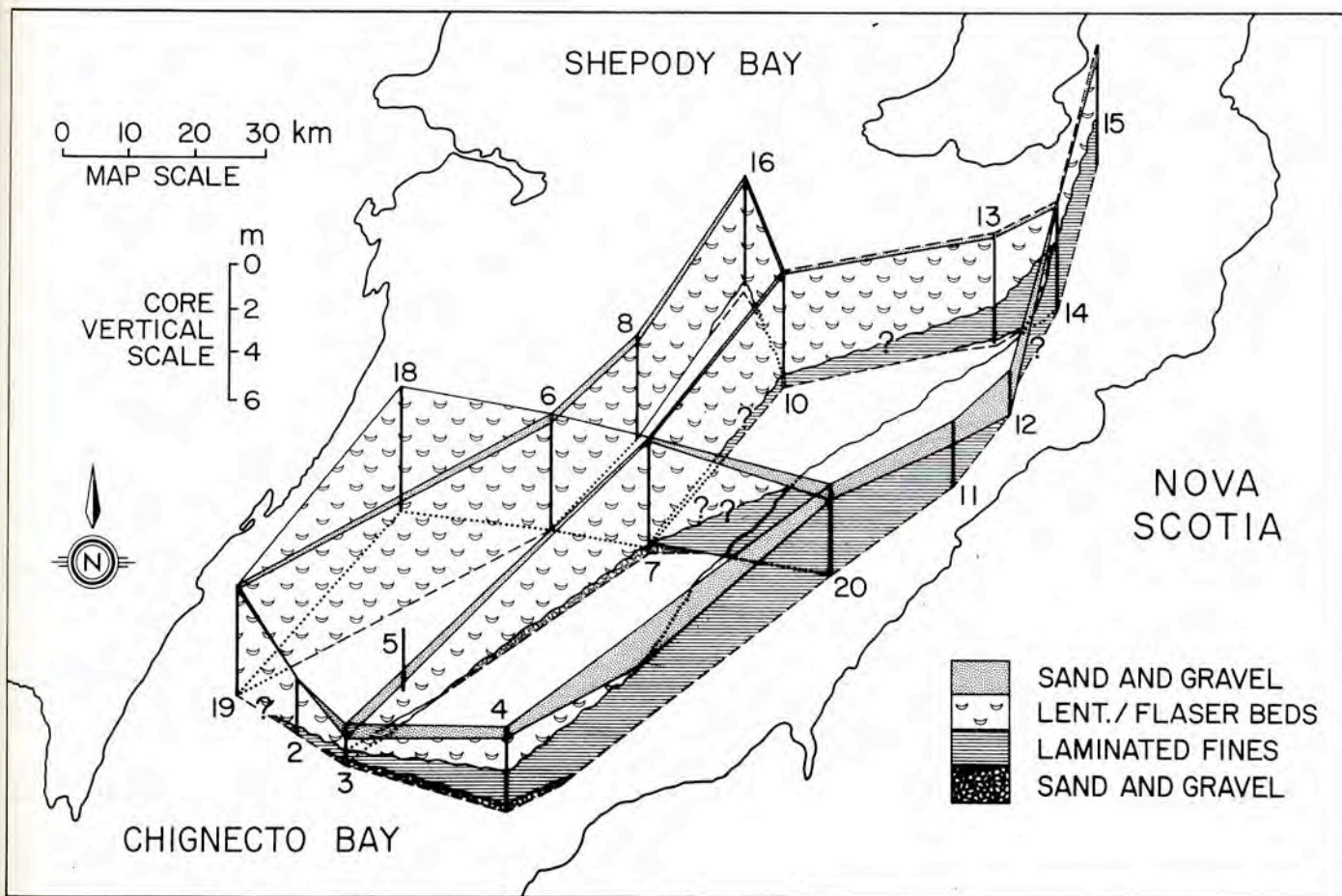


Figure 29. A 3-dimensional fence diagram of the facies distribution in unconsolidated sediments from inner Chignecto Bay, based on the examination of 16 vibracores. The facies show an asymmetrical distribution across the estuary. Laminated sand/fines prevail in the eastern side of the bay, whereas lenticular and flaser bedding prevail in the west. Modern sediments (sand and gravel) predominate in the eastern part of the bay due to a local supply (cliff erosion) of this material. Note that the sands on the eastern side of the bay are not resolved acoustically from the underlying units (G2).

head of Chignecto Bay by Dewolfe *et al.* (1990) show few areas of net accumulation. Seabed reworking introduces a further  $6.0 \times 10^6 \text{ m}^3/\text{a}$  of fine grained sediment into suspension. Fines are, therefore, presumed to be exported to the Bay of Fundy at the rate of input from the rivers, cliffs and the seabed ( $7.3 \times 10^6 \text{ m}^3/\text{a}$ ). This export was verified by direct measurements made by Amos and Asprey (1981) at the mouth of Chignecto Bay.

Bedload transport takes place at the margins of Chignecto Bay and along the median lines of Shepody Bay and Cumberland Basin. In all cases, the direction of transport is headward. Residual transport of suspended sediment in the inner bay is complex, and can reverse direction through time. Such reversals maintain an equilibrium suspended mass in the system and an equilibrium down-estuary concentration gradient.

#### ACKNOWLEDGMENTS

These data were collected in cooperation with D. C. Gordon (D.F.O.) and G. R. Daborn (Acadia University) with sup-

port from K. W. Asprey, D. Beaver, R. B. Murphy and F. Jodrey of the Atlantic Geoscience Centre. Data reduction and plotting were carried out by L. P. Hildebrand, E. B. MacDormand, D. R. Nelson, C. G. Powell, N. A. Rodgers and J. A. Walker. Anchor station data were collected with the support of the officers and crew of CSS Dawson. Interpretation of the surficial sequence was made possible through discussions with R. W. Dalrymple. The updated bathymetry of Chignecto Bay was provided courtesy of the Canadian Hydrographic Service. The two waveriders were maintained and serviced, and the data processed by the Wave Climate Group (Marine Environmental Data Services, Ottawa). Stream gauging results and fluvial water samples were collected by Inland Waters, Dartmouth, courtesy of D. McBride. This work was carried out under Geological Survey of Canada Project number 780022.

#### REFERENCES

Admiralty Survey 1861. Unpublished Field Sheets, British Admiralty, Admiralty House, Taunton, United Kingdom.

- Amos, C. L. 1984. An overview of sedimentological research in the Bay of Fundy. *In: Update on the marine environmental consequences of tidal power development in the upper reaches of the Bay of Fundy*, D. C. Gordon and M. J. Dadswell (eds.). Canadian Technical Report of Fisheries and Aquatic Sciences, v. 1256, p. 31-43.
- \_\_\_\_\_. 1987. Fine-grained sediment transport in Chignecto Bay, Bay of Fundy, Canada. *Continental Shelf Research*, v. 7, p. 1295-1300.
- \_\_\_\_\_. and Asprey, K. W. 1979. Geophysical and sedimentary studies in the Chignecto Bay system, Bay of Fundy — a progress report. *In: Current Research, Part B*, Geological Survey of Canada, Paper 79-1B, p. 245-252.
- \_\_\_\_\_. and \_\_\_\_\_. 1981. An interpretation of oceanographic and sediment data from the upper Bay of Fundy. *Bedford Institute of Oceanography Report Series BI-R-81-15*, 143 p.
- \_\_\_\_\_. , Buckley, D. E., Daborn, G. R., Dalrymple, R. W., McCann, S. B. and Risk, M. J. 1980. Geomorphology and sedimentology of the Bay of Fundy. *Geological Association of Canada Field Trip Guidebook*, v. 23, 82 p.
- \_\_\_\_\_. and Long, B. F. N. 1980. The sedimentary character of the Minas Basin, Bay of Fundy. *In: The Coastline of Canada*, S. B. McCann (ed.). Geological Survey of Canada Paper 80-10, p. 123-152.
- \_\_\_\_\_. and King, E. L. 1984. Bedforms of the Canadian eastern seaboard: a comparison with global occurrences. *Marine Geology*, v. 57, 167-208.
- \_\_\_\_\_. and Tee, K. T. 1989. Suspended sediment transport processes in Cumberland Basin, Bay of Fundy. *Journal of Geophysical Research*, v. 94(C10), p. 14,407-14,417.
- \_\_\_\_\_. and Topliss, B. J. 1985. Discrimination of suspended particulate matter in the Bay of Fundy using the NIMBUS-7 Coastal Zone Color Scanner. *Canadian Journal of Remote Sensing*, v. 11(1) p. 85-92.
- \_\_\_\_\_. and Zaitlin, B. A. 1985. The effect of changes in tidal range on a sublittoral macrotidal sequence, Bay of Fundy, Canada. *Geo-Marine Letters*, v. 4, p. 161-169.
- Anderton, R. 1985. Clastic facies models and facies analysis. *In: Sedimentology, Recent Developments and Applied Aspects*, P. J. Brenchley and B. P. J. Williams (eds.). Blackwell Scientific Publications, 31-47.
- Bay of Fundy Tidal Power Review Board, 1977. Reassessment of Fundy tidal power: Reports of the Bay of Fundy Tidal Power Review Board and Management Committee. Published by Thorn Press Limited, 516 p.
- Bray, D. I., Demarchant, D. P. and Sullivan, D. L. 1982. Some hydrotechnical problems related to the construction of a causeway in the estuary of the Petitcodiac River, New Brunswick. *Canadian Journal of Civil Engineering*, v. 9, p. 296-307.
- Canadian Hydrographic Survey, 1979. Unpublished Field Sheets, Bedford Institute of Oceanography, Dartmouth, Nova Scotia, Canada.
- Chalmers, R. 1894. Report on the surficial geology of eastern New Brunswick, north-western Nova Scotia and a portion of Prince Edward Island. *Geological Survey of Canada Annual Report*, v. 7, p. 124-131.
- Curry, J. R. 1960. Sediments and history of Holocene transgression, continental shelf, northwest Gulf of Mexico. *In: Recent Sediments, northwest Gulf of Mexico*, F. B. Phleger and T. H. Van Andel (eds.). American Association of Petroleum Geologists, p. 221-226.
- Dalrymple, R. W., Amos, C. L. and McCann, S. B. 1983. Beach and near-shore depositional environments of the Bay of Fundy and southern Gulf of St. Lawrence. *International Association of Sedimentologists, Excursion 6A*, 116 p.
- \_\_\_\_\_. , Makino, Y. and Zaitlin, B. A. (*this volume*). Temporal and spatial patterns of rhythmic deposition on mud flats in the macrotidal Cobequid Bay-Salmon River estuary, Bay of Fundy, Canada. *In: Clastic Tidal Sedimentology*. Canadian Society of Petroleum Geologists, Memoir 16.
- deMargerie, S. and deWolfe, D. 1987. Development of a hydrodynamic model in Cumberland Basin for tidal power applications. Consultant Report prepared by ASA Consulting Ltd., Dartmouth, submitted to Department of Supply and Services, Dartmouth; 98 p.
- deWolfe, D., MacNeil, M., deMargerie, S., Willis, D., Christian, H. and Amos, C. 1990. Sediment transport in Cumberland Basin — Field program data report. Consultant Report prepared by ASA Consulting Ltd., Dartmouth, submitted to Nova Scotia Tidal Power Corporation; 77 p.
- Fader, G. B., King, L. H. and MacLean, B. 1977. Surficial geology of the eastern Gulf of Maine and Bay of Fundy. *Geological Survey of Canada, Paper 76-17*, 23 p.
- Garrett, C. J. R. 1972. Tidal resonance in the Bay of Fundy and Gulf of Maine. *Nature*, v. 283, p. 441-443.
- \_\_\_\_\_. , Keeley, J. R. and Greenberg, D. A. 1978. Tidal mixing versus thermal stratification in the Bay of Fundy and Gulf of Maine. *Atmosphere and Oceans*, v. 16(4), p. 403-423.
- Godin, G. 1968. The 1965 current survey of the Bay of Fundy — a new analysis of the data and the interpretation of the results. *Marine Sciences Directorate Report*, Ottawa, no. 8, 96 p.
- \_\_\_\_\_. 1980. Cotidal charts for Canada. *Marine Sciences Directorate Report*, Ottawa, no. 55, 93 p.
- Goldthwait, J. W. 1924. *Physiography of Nova Scotia*. Geological Survey of Canada, Memoir 140, 179 p.
- Gordon, D. C. and Desplanque, C. 1983. Dynamics and environmental effects of ice in the Cumberland Basin of the Bay of Fundy. *Canadian Journal of Fisheries and Aquatic Sciences*, v. 40(9), p. 1331-1342.
- \_\_\_\_\_. and Dadswell, M. J. 1984. Update on the marine environmental consequences of tidal power development in the upper reaches of the Bay of Fundy. *Canadian Technical Report of Fisheries and Aquatic Sciences*, v. 1256, 686 p.
- Grant, D. R. 1970. Recent coastal submergence of the Maritime Provinces, Canada. *Canadian Journal of Earth Sciences*, v. 7, p. 676-689.
- Grant, D. R. 1985. Glaciers, sediment and sea-level; northern Bay of Fundy, N.S. 14th Arctic Workshop, Nova Scotia Field Trip B, 36 p.
- Greenberg, D. A. 1983. Modeling the mean barotropic circulation in the Bay of Fundy and Gulf of Maine. *Journal of Physical Oceanography*, v. 13, p. 886-904.
- Harrison, W. and Lyon, C. J. 1963. Sea-level and crustal movements along the New England-Adian shore, 4,500-3,000 B.P. *Journal of Geology*, v. 71(1), p. 96-108.
- Hildebrand, L. P., MacDormand, E. B., Nelson, D. R., Powell, C. G., Rodgers, N. A. and Walker, J. A. 1980. Activities of the Job Corps Program; Fundy Tidal Power Development. National Research Council of Canada, Halifax, Project 16-01-002N, 176 p.
- Holloway, P. E. 1981. Longitudinal mixing in the upper reaches of the Bay of Fundy. *Estuarine Coastal and Shelf Sciences*, v. 13, p. 495-515.
- Hussain, M. 1980. Textural and mineralogical analysis of Chignecto Bay sediments, Canada. Unpublished M. Sc. Thesis, Acadia University, 138 p.
- Keizer, P. D., Gordon, D. C. and Hayes, E. R. 1984. A brief overview of recent research in the Bay of Fundy. *In: Update on the marine environmental consequences of tidal power development in the upper reaches of the Bay of Fundy*, D. C. Gordon and M. J. Dadswell (eds.). Canadian Technical Report of Fisheries and Aquatic Sciences, v. 1256, p. 45-63.
- King, L. H. and MacLean, B. 1976. Geology of the Scotian Shelf and adjacent areas. *Marine Sciences Paper no. 7*, Geological Survey of Canada, Paper 74-31, 31 p.
- Klein, G. deV. 1970. Depositional and dispersal dynamics of intertidal sand bars. *Journal of Sedimentary Petrology* 40, 1095-1127.
- Laming, D. J. C. 1967. Sediment movement in Chignecto Bay. Unpublished report to Atlantic Tidal Power Programming Board, May, 1967, 26 p.
- Lewis, P. J. and Moran, M. D. 1984. Severe storms off Canada's east coast: a catalogue summary for the period 1957 to 1983. *Canadian Climate Centre Report*, 84-13, C1.3 p.
- Loring, D. H. 1982. Geochemical factors controlling the accumulation and dispersal of heavy metals in the Bay of Fundy sediments. *Canadian Journal of Earth Sciences*, v. 19(5), p. 930-944.
- Lougee, R. J. 1953. A chronology of post-glacial time in eastern North America. *Scientific Monthly*, v. 76, p. 259-276.
- Marine Environmental Data Services, 1979(a). Waves recorded off Shepody Bay, N.B., June 14, 1978 to December 13, 1978: Unpublished Report of Wave Climate Group, Ottawa, no. 146-1m.
- \_\_\_\_\_. 1979(b). Waves recorded off Cape Enragé, Chignecto Bay, June 13, 1978 to April 20, 1979. Unpublished Report of Wave Climate Group, Ottawa, no. 147-1m.
- Milliman, J. D. and Enory, K. O. 1968. Sea levels during the past 35,000 years. *Science*, v. 162, p. 1121-1123.
- Munday, J. C., Alfoldi, T. T. and Amos, C. L. 1980. Application of a system for automated multitime Landsat measurement of suspended sediment. *Water Quality Bulletin*, v. 5(1), p. 6-10.
- Nio, S-D and Yang, C-S. 1989. Recognition of tidally-influenced facies and environments. Short course notes, series #1, International Geoservices BV, Leiderdorp, The Netherlands, 230 p.
- \_\_\_\_\_. (*this volume*). Diagnostic attributes of clastic tidal deposits: a review. *In: Clastic Tidal Sedimentology*, Canadian Society of Petroleum Geologists, Memoir 16.
- Noordijk, A. and Pronk, T. 1981. De Holocene afzettingen in de dalen van de Missiguash, La Planche, en Nappan, Bay of Fundy, Canada: Unpublished Ph.D. Thesis, Free University, Amsterdam, 65 p.

- Pelletier, B. R. and McMullen, R. M. 1972. Sedimentation patterns in the Bay of Fundy and Minas Basin. *In: Tidal Power*, T. J. Gray and O. K. Gashus (eds.). Plenum Publishing Corporation, New York, p. 153-187.
- Poole, W. H., Sanford, B. V., Williams, H. and Kelley, D. G. 1976. Geology of southeastern Canada. *In: Geology and Economic Minerals of Canada*, R. J. W. Douglas (ed.). Geological Survey of Canada, p. 227-304.
- Pritchard, D. W. 1956. The dynamic structure of a coastal plain estuary. *Journal of Marine Research*, v. 15, p. 33-42.
- Quinlan, G. and Beaumont, C. 1982. The deglaciation of Atlantic Canada as reconstructed from the postglacial relative sea-level record. *Canadian Journal of Earth Sciences*, v. 19, p. 2232-2246.
- Rampton, V. N., Gauthier, R. C., Thibault, J. and Seaman, A. A. 1984. Quaternary geology of New Brunswick. Geological Survey of Canada, Memoir, v. 416, 77 p.
- Schubel, J. R. and Carter, H. H. 1984. The estuary as a filter for fine-grained suspended sediment. *In: The Estuary as a Filter*, V. S. Kennedy (ed.). Academic Press, San Diego, p. 81-105.
- Scott, D. B. and Greenberg, D. A. 1983. Relative sea-level rise and tidal development in the Fundy tidal system: *Canadian Journal of Earth Sciences*, v. 20(10), p. 1554-1564.
- \_\_\_\_\_ and Medioli, F. S. 1980. Post-glacial emergence curves in the Maritimes determined from marine sediments in raised basins. *Proceedings of the Canadian Coastal Conference*, Burlington, p. 428-446.
- Smith, D. G. 1989. Comparative sedimentology of mesotidal (2 to 4 m) estuarine channel point bar deposits from modern examples and ancient Athabasca oil sands (Lower Cretaceous), McMurray Formation. *In: Modern and Ancient Examples of Clastic Tidal Deposits — A Core and Peel Workshop*, G. E. Reinson (ed.). Canadian Society of Petroleum Geologists, Special Publication S 31, p. 60-65.
- Stephens, G. R. 1977. Geology and tectonic framework of the Bay of Fundy — Gulf of Maine region. *In: Fundy Tidal Power and the Environment*, G. R. Daborn (ed.). Acadia University Institute, Publication no. 28, p. 82-100.
- Stravers, J. A. and Syvitski, J. P. M. (*in press*). Early Holocene land-sea correlations and deglacial evolution of the Cambridge Fiord Basin, northern Baffin Island. *Quaternary Research*.
- Swift, D. J. P. and Lyall, A. K. 1968. Origin of the Bay of Fundy. *Marine Geology*, v. 6, p. 331-343.
- \_\_\_\_\_, Pelletier, B. R., Lyall, A. K. and Miller, J. A. 1973. Quaternary sedimentation in the Bay of Fundy. Geological Survey of Canada, Paper 71-23, p. 113-151.
- Syvitski, J. P. M., Beattie, D. D., Praeg, D. B. and Schaffer, C. T. 1987. Marine Geology of Baie des Chaleurs. Geological Survey of Canada Open File 1375.
- Taylor, R. B., Praeg, D. B. and Syvitski, J. P. M. 1987. Coastal morphology and sedimentation, eastern Baffin and Bylot Islands, NWT. *In: Sedimentology of Arctic fjords experiment*, Data report, volume 3, J. P. M. Syvitski and D. B. Praeg (eds.). Canadian Data Report of Hydrography and Ocean Sciences 54, p. 3-1 — 3-60.
- Tee, K. T. 1982. The structure of the three-dimensional tide-generating currents: experimental verification of a theoretical model. *Estuarine, Coastal and Shelf Science*, v. 14, p. 27-48.
- Tee, K. T. and Amos, C. L. (*in press*). Tidal and buoyancy driven currents in Chignecto Bay, Bay of Fundy. *Journal of Geophysical Research*.
- Terwindt, J. H. J. 1981. Origin and sequences of sedimentary structures in inshore mesotidal deposits of the North Sea. *International Association of Sedimentologists, Special Issue*, 5, p. 4-26.
- Topliss, B. J., Amos, C. L. and Hill, P. R. 1990. Algorithms for remote sensing of high concentration, inorganic suspended sediment. *International Journal of Remote Sensing* 11(6), p. 947-966.
- Wagner, F. J. E. 1980. A faunal interpretation of tidal evolution in Minas Basin, Nova Scotia. *Géographie, Physique et Quaternaire*, v. 34, p. 253-257.
- Williams, H., Kennedy, J. J. and Neale, E. R. W. 1972. The Appalachian structural province. *In: Variations in tectonic style in Canada*, L. A. Price and R. J. W. Douglas (eds.). v. II, p. 181-261.
- Wightman, D. M. and Cooke, H. B. S. 1978. Postglacial emergence in Atlantic Canada. *Geoscience Canada*, v. 5, p. 61-65.

KEY WORDS: MACROTIDAL, MESOTIDAL, TURBID, ESTUARINE, SEDIMENT BUDGET, GLACIAL